Title: Flexible Energy Storage Systems Based on Electrically Conductive Hydrogels

Authors: Wei Zhang, Pan Feng, Jian Chen, Zhengming Sun, Boxin Zhao

PII: S0079-6700(18)30196-5
DOI: https://doi.org/10.1016/j.progpolymsci.2018.09.001
Reference: JPPS 1102

To appear in: *Progress in Polymer Science*

Received date: 8-6-2018
Revised date: 31-8-2018
Accepted date: 1-9-2018

Please cite this article as: Zhang W, Feng P, Chen J, Sun Z, Zhao B, Flexible Energy Storage Systems Based on Electrically Conductive Hydrogels, *Progress in Polymer Science* (2018), https://doi.org/10.1016/j.progpolymsci.2018.09.001

Flexible Energy Storage Systems Based on Electrically Conductive Hydrogels

Wei Zhang[1,*], Pan Feng[1], Jian Chen[1,*], Zhengming Sun[1], Boxin Zhao[2,3,4]

[1]School of Materials Science and Engineering, Jiangsu Key Laboratory for Advanced Metallic Materials, Southeast University, China
[2]Department of Chemical Engineering, [3]Waterloo Institute for Nanotechnology, [4]Institute for Polymer Research, University of Waterloo, 200 University Avenue West, Waterloo, Ontario, Canada N2L 3G1

*Corresponding Authors: w69zhang@seu.edu.cn (Wei Zhang); j.chen@seu.edu.cn (Jian Chen)

Graphical abstract

Graphical abstract: Electrically conductive hydrogels (ECHs), combining electrical properties of metals or semiconductors with the unique features of hydrogels, are ideal frameworks to design and construct flexible supercapacitors and batteries. This review summarized the material design and synthetic approach of ECHs, demonstrating the advances of percolation theory in ECH materials, followed by presenting their effective application in flexible energy storage systems, and discussed the challenges and opportunities in this field.

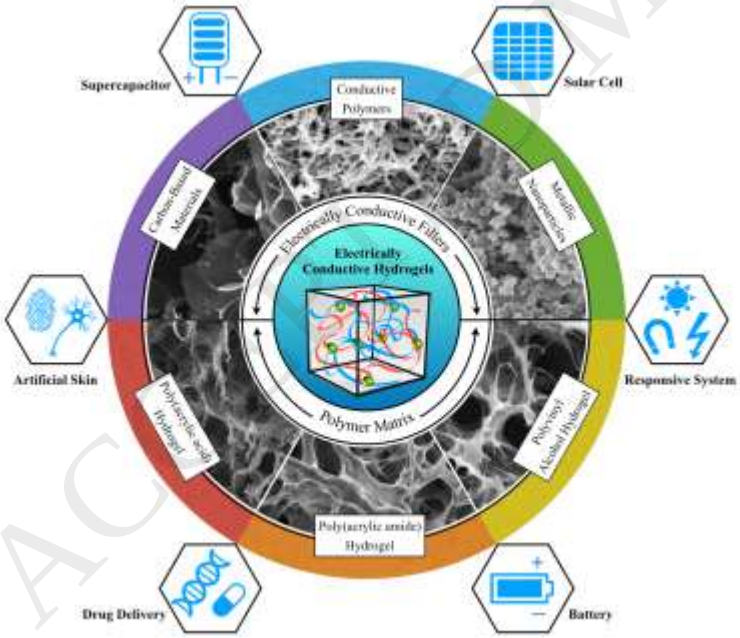

Abstract

To power wearable electronic devices, various flexible energy storage systems have been designed to work in consecutive bending, stretching and even twisting conditions. Supercapacitors and batteries have been considered as the most promising energy/power sources for wearable electronics; however, they need to be electrochemically sustainable and mechanically robust. Electrically conductive hydrogels (ECHs), combining electrical properties of metals or semiconductors with the unique features of hydrogels, are ideal frameworks to design and construct flexible supercapacitors and batteries. ECHs are intrinsically flexible to sustain large mechanical deformation, they can hold a large amount of electrolyte solution in a 3D nanostructured conducting network, providing an extremely high surface area for the required electrochemical reactions. To date, nanostructured three-dimensional ECHs have exhibited high performance when applied as active electrode materials for supercapacitors and lithium-ion batteries. Future efforts lie in the development of functional ECHs with controllable size, composition, morphology, and interface. This review summarized the material design and synthetic approach of ECHs, demonstrating the advances of percolation theory in ECH materials, followed by presenting their effective application in flexible energy storage systems, and discussed the challenges and opportunities in this field.

Keywords: Electrically conductive hydrogel; Conductive polymer; Flexible electrode; Supercapacitor; Lithium-ion battery

1. Introduction

Gel can be considered as an elastic crosslinked polymer network filled with plenty of fluid.[1–4] Hydrogel is composed of “hydro” (water) and ‘‘gel’’; therefore, it is an aqueous gel which can hold a large amount of water and swell to an equilibrium volume in its three-dimensional network.[5–7] The ability of swelling and retaining a significant fraction of water is due to the hydrophilic functional groups attached to the hydrogel polymeric backbone; while the resistance to dissolution can be attributed to the crosslinked hydrogel network, where cohesive forces generated by covalent bonds between the polymer chains prevent further penetration of water.[8–11]

Electrically conductive hydrogels (ECHs) are an emerging class of hydrogels combining a hydrophilic matrix with electrically conductive fillers, such as metallic nanoparticles, conductive polymers (CPs), or carbon-based materials.[3,4,12] With the reversible capability between swelling and de-swelling, ECHs can be designed to perform dramatic liquid exchange or volume transition with controllable responses to extensive environmental conditions, such as electric or magnetic field, light, and ionic conductivity.[13–15] As a result, ECHs have exceptional promises in many applications, ranging from renewable energy[16–19], flexible electronics[20–22], and

environmental engineering[23–25] to medical devices[26–28] and drug delivery systems[8,29–31]. Figure 1 summarizes some application areas with the typical examples of ECHs.

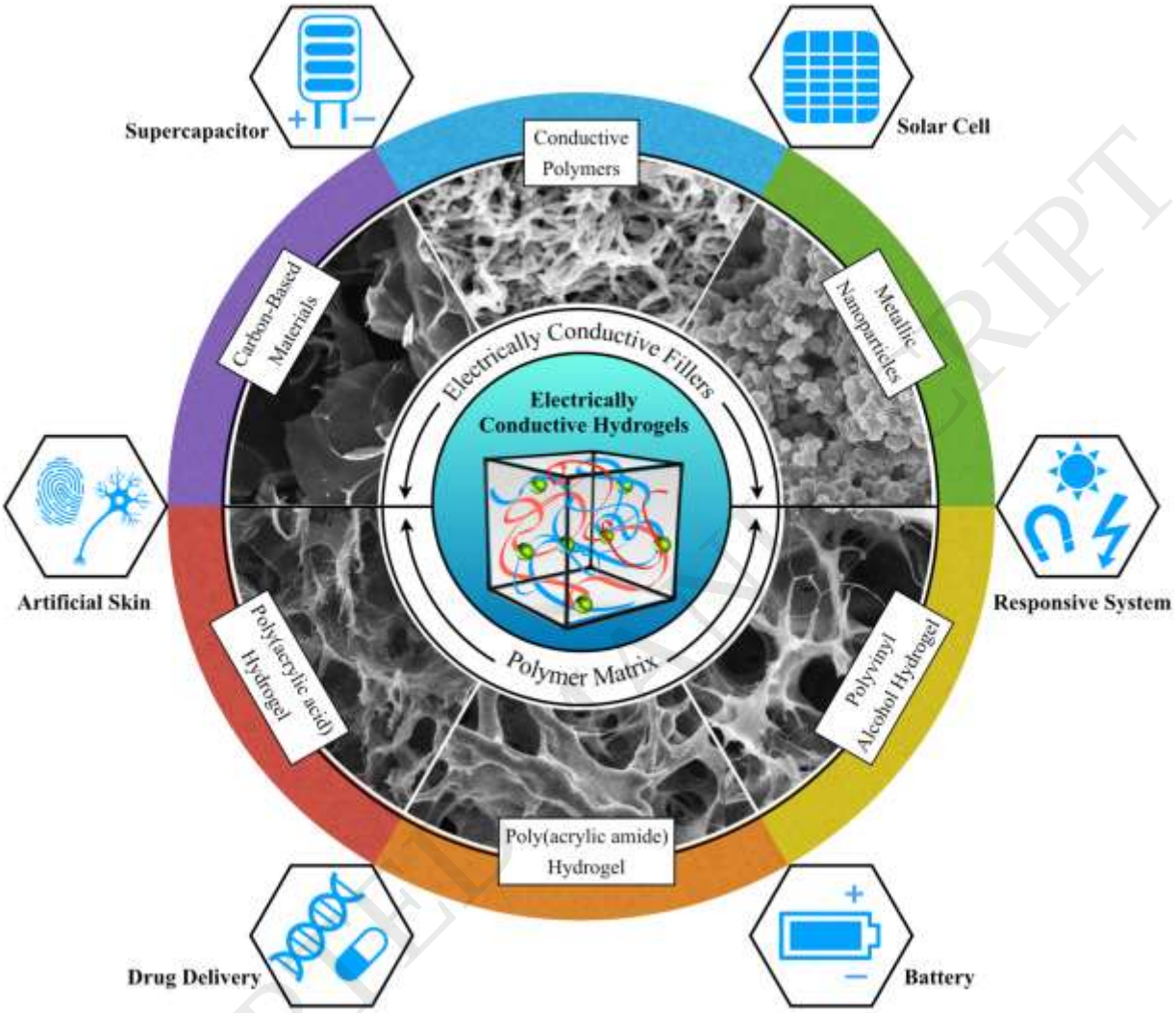

Figure 1. Electrically conductive hydrogels are an emerging class of hydrogels combining a hydrophilic matrix with conductive fillers, and they have exceptional promises in a wide range of applications.

To power wearable electronic devices, various flexible energy storage systems have been designed to work in consecutive bending, stretching and even twisting conditions. Supercapacitors and batteries are under serious consideration as a promising flexible energy storage device, as long as they are constructed to be electrochemically sustainable and mechanically robust.[32–35] Despite the different energy storage mechanisms, supercapacitors and batteries share some "electrochemical similarities".[36–39] For instance, both of their electrochemical reactions occur at the electrode/electrolyte interface, and their electron and ion transport are separated,[36,40] thus an active interface between the electronic-transporting phase (electrode materials) and the ionic-transporting phase (electrolyte solution) at the molecular level is highly desirable. Moreover, the performance of a flexible supercapacitor or battery strongly depends on the properties of electrode materials,[41–44] which have to be electrochemically active and inherently soft. With this regard,

ECHs have been explored as a potential platform to design and construct flexible supercapacitors and batteries,[45–47] because this "aqueous soft material" synergizes the advantages of hydrogels and electron conductors, possesses high electrical conductivity and mechanical flexibility, superior electron and ion transportation, and effective interfacial interaction between solid and solution phases.

Considerable progress in this field has been made to the development of ECHs for flexible energy storage applications.[46,48,49–56,57] In this review, various synthetic approaches and fabrication techniques of ECHs are presented, which will hopefully provide a guideline for designing hydrogels with desired properties. The state-of-the-art applications of ECHs in flexible supercapacitors and batteries, and the challenges in developing these materials are discussed in parallel.

2. Material Design and Synthetic Approach

Thus far, a diverse range of ECHs have been developed by combining various conductive components and different types of polymer matrix,[3,26,33,58–60] while the conductive fillers bring electrical conductivity to the scaffold, and the conventional insulating polymers provide the structural support of the ECHs. A schematic illustration of four synthetic approaches of ECHs is presented in Figure 2, they can be prepared by either gelation from a conductive particles suspension or in-situ polymerization within a preformed hydrogel. Alternatively, conductive polymers or graphene can also be crosslinked directly as the main continuous phase of the hydrogel structure. The approach chosen will be, in part, determined by the nature of conductive fillers and the intended applications of ECHs.

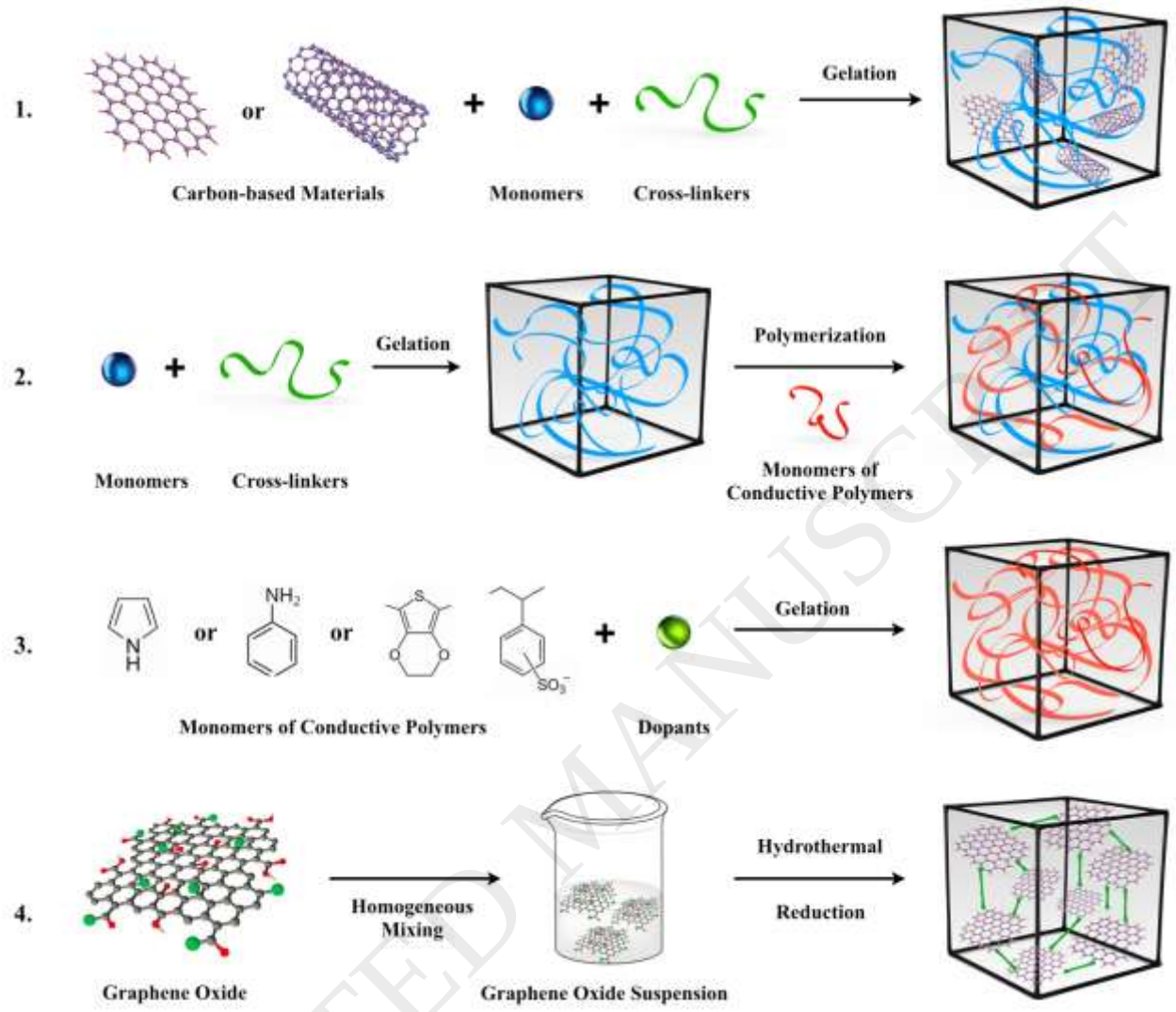

Figure 2. Four main approaches used to obtain ECHs: (1) Hydrogel formation from a conductive filler suspension; (2) polymerization within a preformed hydrogel matrix; (3) crosslinking conductive polymers by dopant molecules; (4) self-assembly of graphene hydrogel via supramolecular interactions.

2.1 Hydrogel Formation from a Conductive Filler Suspension

One of the simplest approach to form an ECH is the gelation of hydrogel monomer in a suspension of conductive fillers, such as carbon-based materials,[24,34,61,62] metallic nanoparticles,[63–65] and conductive polymers.[50,60,66–68] Graphene and carbon nanotubes have been widely implemented as fillers to improve mechanical properties of the polymer composite, while bringing electrical conductivity to the system.[69–71] As such, they are also commonly used conductive fillers for the preparation of ECHs via this approach (Figure 2, Approach 1).

In a typical synthesis, graphene oxide (GO)/poly(acrylic acid) (PAA) hydrogel was prepared by adding initiator to a solution consisting of hydrogel monomer, crosslinker and graphene oxide (GO), followed by free-radical polymerization initiated by heat.[61] The functional groups on GO

not only make them thoroughly exfoliated in water, also provide hydrogen bonding with PAA to improve the mechanical strength of GO/PAA hydrogels. Other hydrogel matrixes such as poly (N-isopropylacrylamide) (PNIPAM),[72] poly(acrylic amide) (PAM),[73] and polyvinyl alcohol (PVA) have also been used to prepare composite hydrogels.[23]

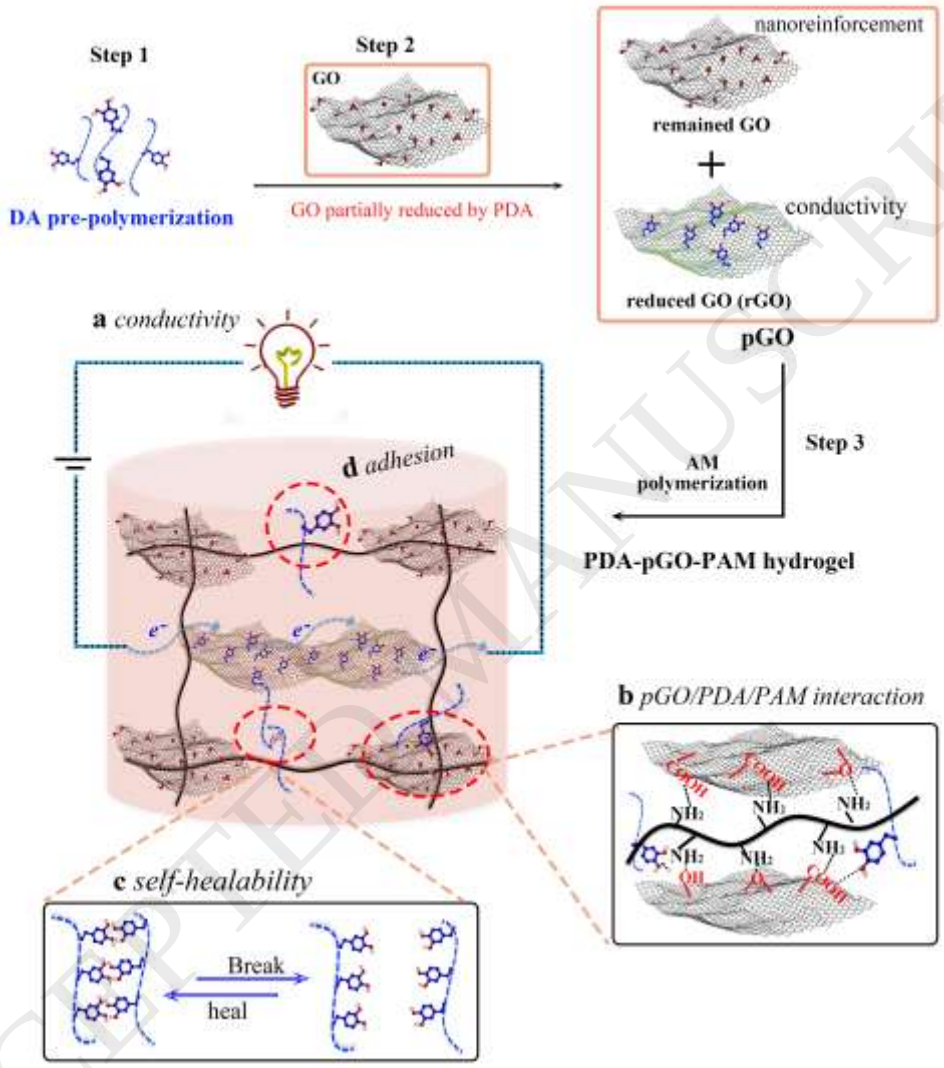

Figure 3. Schematic of mussel-inspired PDA-rGO/PAM hydrogel. Step 1: dopamine pre-polymerization; Step 2: GO was partially reduced to form rGO; Step 3: polymerization of acrylamide monomers. Adapted with permission from Ref. 73. Copyright © 2017 Wiley-VCH Verlag GmbH & Co. KGaA, Weinheim.

Heavy oxidation of GO could decrease their conductivity by creating too many disorder sites.[69] To enhance the electrochemical properties of the GO hydrogels, a reported strategy is to reduce GO during the gel synthesis, Lu *et al*. implemented GO via PDA modification to fabricate a hydrogel simultaneously possessing high conductivity and toughness, as well as self-adhesiveness and self-healability.[73] Such ECH was synthesized by partially converting GO to reduced graphene oxide (rGO) through polydopamine (PDA) reduction, followed by the polymerization of

acrylamide (AM) monomers at the presence of initiator and crosslinker (Figure 3). Mussel-inspired PDA coating has been widely exploited as a versatile surface modification strategy, which in this work has been used to functionalize rGO, and make it well dispersed in the hydrogel network to provide effective electronic pathway.

In a similar strategy, Zhang *et al*. used PDA to modify the surface properties of single-wall carbon nanotubes (CNTs),[16] facilitating its uniform distribution in the PVA solution, consequently leading to a novel ECH crosslinked via supramolecular interactions. In this approach, carbon-based materials only act as conductive fillers rather than crosslinking agents, thus a stable interconnected polymer chain was necessary to provide structural support. Therefore, the key of this approach relies on good dispersion of conductive fillers in pre-gelled solution, and subsequently in the 3D hydrogel network.

2.2 Polymerization within a Preformed Hydrogel Matrix

The design and fabrication of double network hydrogels has enabled this two-step preparation method,[25,74,75] through which the first non-conductive hydrogel network is preformed and acts as the supporting framework for in situ polymerization of the second conductive polymeric network (Figure 2, Approach 2).

The first ECH synthesized by this approach was reported in 1994 by Gilmore *et al*.,[76] who polymerized polypyrrole (PPy) directly on a preformed PAM hydrogel. This work has inspired the fabrication of ECHs from different combinations of many available hydrogels (PAM, PAA, PVA, agarose and chitosan) and a range of CPs (polypyrrole, polyaniline, and polyethylenedioxy thiopehene).[13,15,27,32,59,72,77,78]

In a study reported by Ambrosio *et al*.,[27] aniline monomer was first dissolved in polyethylenglicole diacrylate (PEGDA) solution; then UV photopolymerization was performed to construct a crosslinked hydrogel network with a super-porous architecture. Another ECH example is the polyaniline (PANI)/heparin-methacrylate hydrogel, its synthetic approach is demonstrated in Figure 4.[28] At first, a biologically derived heparin hydrogel network was formed by UV curing; it was then soaked in an aniline solution to allow monomer to diffuse into the porous structure. At the end, PANI/heparin-methacrylate hydrogel was formed by oxidative polymerization of aniline and physically entrapped PANI within the heparin-methacrylate hydrogel matrix.

In a similar mechanism, Yaszemski *et al*. extended this methodology to the fabrication of a composite ECH consisting of oligo(polyethylene glycol fumarate) (OPF) and PPy.[78] OPF hydrogel was first synthesized based on the reaction of fumaryl chloride and polyethylene glycol to serve as the polymer matrix, in which pyrrole was chemically grown via free radical polymerization. This approach presents a facile and versatile fabrication technique for ECHs, by

choosing proper polymer matrix and conductive polymers; as-obtained hydrogels exhibited desired mechanical strength and electrical conductivity.

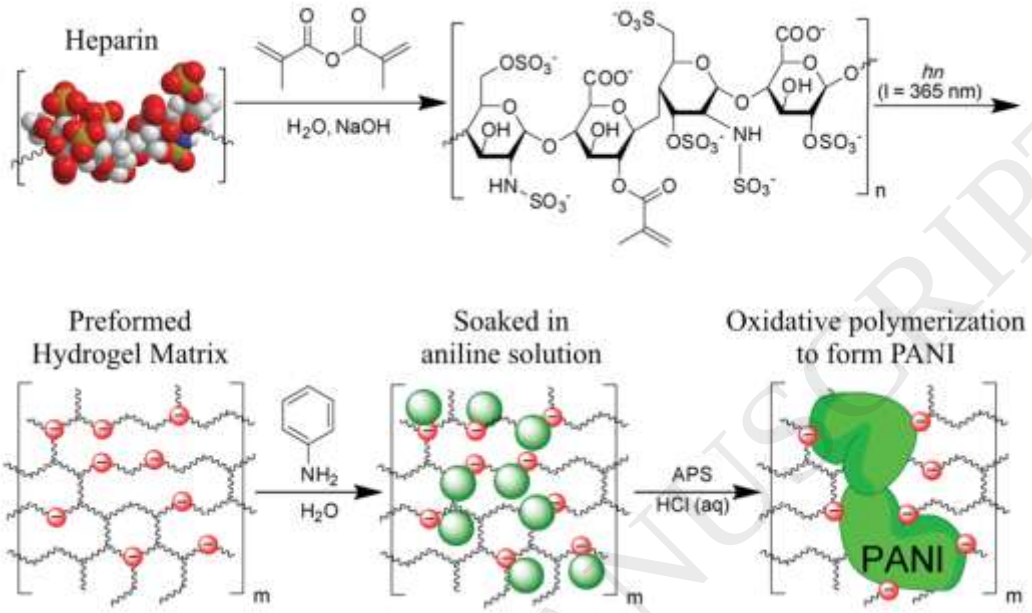

Figure 4. Synthetic approach of heparin-methacrylate/PANI hydrogel. Adapted with permission from Ref. 28. Copyright © 2014 American Chemical Society.

2.3 Crosslinking Conductive Polymers by Dopant Molecules

The two ECH preparation methods discussed in section 2.1 and 2.2 both require a non-conductive framework to either entrap or support conductive fillers, but these non-conductive polymer matrixes occupy a significant fraction of space in the ECHs, which is inefficient for the final flexible supercapacitor or battery configurations. As a result, many researchers have attempted to crosslink the conductive polymer chains directly to form a 3D hydrogel network without using any insulating polymer matrix (Figure 2, Approach 3).[48,49,79,80]

The first conductive polymer-only hydrogel was prepared by MacDiarmid *et al*.;[81] they observed the gelation process of sufficiently concentrated PANI solutions, which was caused by physical crosslinking of crystalline domains and associated 1-D nematic-type alignment of amorphous PANI. Instead of gelating at high concentration, Bao *et al*. doped PANI with phytic acid and simultaneously gelated the system;[80] the gelation mechanism is schemed in Fig. 5a. By protonating the amino-groups on PANI, each phytic acid molecule can react with several PANI polymer chains, resulting in the crosslinked 3D hierarchical microstructure with the pore sizes ranging from angstrom, nanometer to micron.

PPy is another conductive polymer that has been crosslinked itself to form an ECH. Yu *et al*. applied interfacial polymerization strategy to prepare nanostructured conducting PPy hydrogels at an organic/aqueous biphasic interface.[82] By adjusting the mole ratio of monomer pyrrole to

crosslinker phytic acid, the morphology of prepared PPy hydrogel could be tuned from hollow spherical structure (Py:PA = 5:1) to particle-like hierarchically porous network (Py:PA = 10:1). Besides using phytic acid, the same group changed dopant molecule to copper phthalocyanine-3,4',4'',4'''-tetrasulfonic acid tetrasodium salt (CuPcTs), and synthesized an interconnected PPy fiber structure, which was further crosslinked and gelated into a hydrogel. As shown in Figure 5b, CuPcTs acted as both the dopant and gelator to self-assembled the "necklace-like" 1D PPy nanofiber into 3D hydrogel network through electrostatic interaction and hydrogen bonding.

So far PANI and PPy are the only two conductive polymers that have been found able to be crosslinked by dopant molecules in literatures. The advantage of this approach is to overcome the aforementioned limitations and create a continuous conductive phase in ECHs made from the conjugated polymers, and by employing different conductive polymer monomers and crosslinkers, the morphology of the resulted ECHs can be precisely controlled.

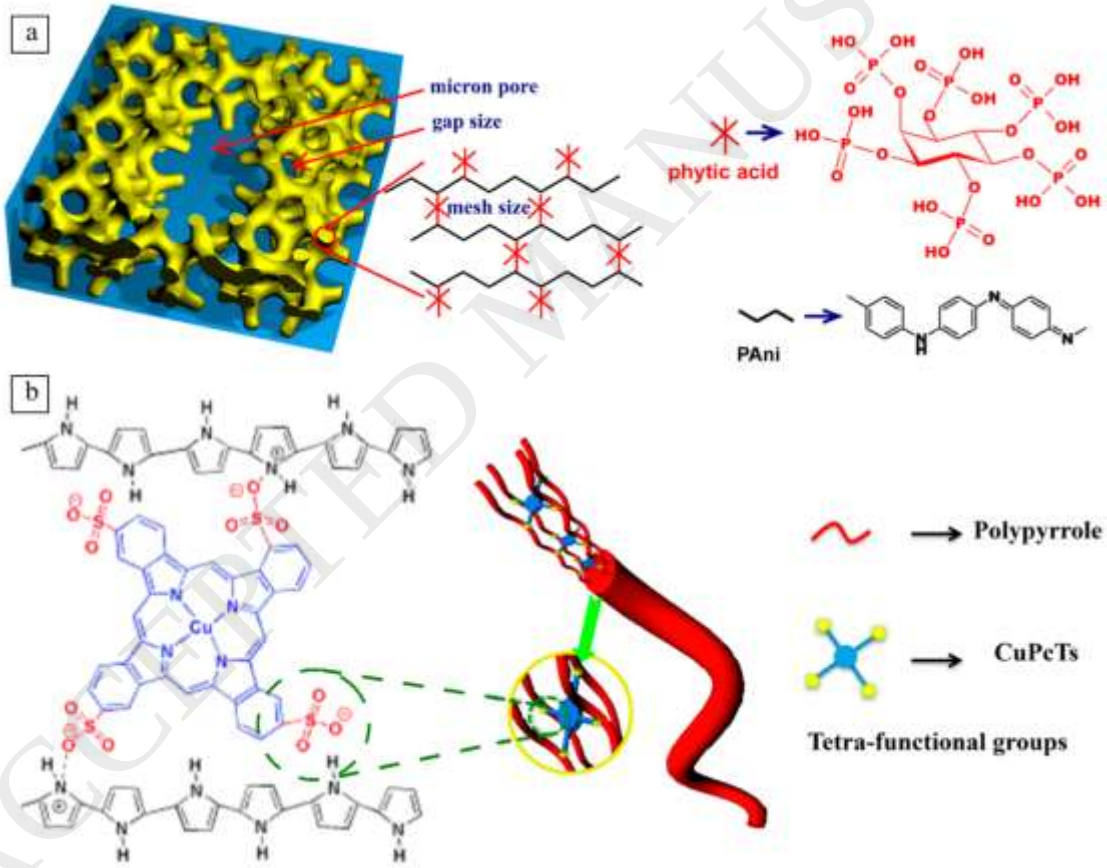

Figure 5. (a) Schematic illustrations of the 3D hierarchical microstructure of the PANI hydrogel. Adapted with permission from Ref. 80. Copyright © 2012 National Academy of Sciences. (b) Controlled synthesis of the CuPcTs doped PPy hydrogel. Adapted with permission from Ref. 82. Copyright © 2015 American Chemical Society.

2.4 Self-assembly of Graphene Hydrogel via Supramolecular Interactions

Similar to conductive polymer-based hydrogels, graphene or its derivatives based ECHs are either a hybrid hydrogel composite, which can be prepared via the approach described in Section 2.1, or a "single component" fabricated by hydrothermal reaction (Figure 2, Approach 4). Hydrothermal synthesis is normally used to prepare graphene-based nanocomposites from high-temperature aqueous solutions at high vapor pressures.[69]

Shi *et al*. first adopted this method to synthesize a self-assembled graphene hydrogel with crosslinked 3D porous structure (Figure 6a).[83] In this one-step process, homogeneous GO suspension was sealed in an autoclave and heated at 180 °C for 12 h without any disturbance, then the autoclave was cooled to room temperature and graphene hydrogel was formed via supramolecular interactions, including hydrogen bonding, electrostatic interaction and π-π stacking (Figure 6b). The properties of the graphene hydrogel are strongly depending on the precursor (GO) concentration during self-assembly process. When at low GO concentration (0.5mg/mL), only black powdery materials were obtained. After increasing GO concentration to 1 or 2 mg/mL, the well-defined graphene hydrogels could be readily constructed (Figure 6c). As-prepared graphene hydrogels can be further treated with hydrazine or hydroiodic acid to remove residual oxygenated groups for improved conductivity.[45]

These studies offer a facile method to construct 3D hydrogel networks from 2D graphene sheets and inspire many novel designs of graphene-based hydrogel systems. For example, Li *et al*. demonstrated the controlled assembly of gold/graphene hydrogels from a suspension of gold nanocrystals and GO layers;[84] Cong *et al*. reduced GO by ferrous ions and simultaneous deposited Fe_3O_4 nanoparticles on graphene sheets, followed by hydrothermal reaction to develop magnetic Fe_3O_4/graphene hydrogels;[85] By pre-mixing GO aqueous dispersion with certain amount of titanium dioxide (TiO_2) nanoparticles, Liu *et al*. developed multifunctional TiO_2/graphene hydrogels through the same hydrothermal reaction.[79] The graphene hydrogels obtained from this approach exhibited well-defined interconnected structure with high mechanical strength (Figure 6d), but they do not contain a hydrophilic polymer matrix, thus lacking the ability of holding a large amount of liquid.

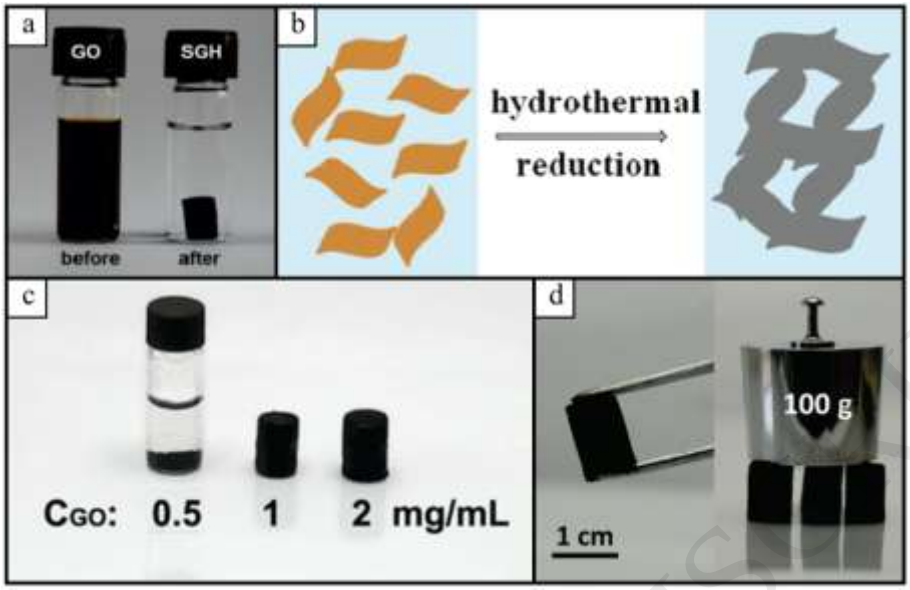

Figure 6. (a) Photograph of GO dispersion before (left) and after hydrothermal reduction (right). (b) The hydrothermal formation mechanism for the graphene hydrogel. (c) Optical images of the graphene hydrogels prepared by hydrothermal reduction at different GO concentration. (d) Optical images of three graphene hydrogel columns holding 100 g weight. Adapted with permission from Ref. 83. Copyright © 2010 American Chemical Society.

3. Percolation Theory in Electrically Conductive Hydrogels

Percolation theory is frequently applied to describe the phase transition phenomenon and electron transfer mechanism in filler-matrix composites.[86–89] Given the fact that ECHs are also filler-matrix composite materials, percolation theory allows to describe and model the effects of conductive fillers on ECH performance, including electrical conductivity and mechanical strength, as well as sol-gel transversion properties.

The percolation mechanism can be explained by Figure 7a, which presents a conceptual graph of three distinct conductance regions of a composite material as a function of the filler concentrations. In the first region, there is almost no conduction due to the insufficient conductive fillers to create effective electron transfer pathway. As the amount of conductive fillers increases and the percolation threshold reaches, a sharp jump of several orders of magnitude in conductivity is observed in the percolation region. When isolated fillers form stable contacts from discrete elements to a compact network, a constant gradient conduction region can be achieved. The exact shape of Figure 7a could be varied depending on different percolation systems, but the general trend will be similar to all filler-matrix systems.[90–93]

In most cases, electrical conductive fillers are added to the non-conductive polymer matrix to provide a three-dimensional electron transfer network throughout the composite.[94–96] When more and more conductive fillers randomly distribute in the polymer network, free overlap, their distance distributions for the critical percolation in an insulating matrix can be simulated as shown

in Figures 7b, the electron transfer paths are marked in black.[94] The formation of these electron transfer paths eventually leads to an insulator-to-conductor transition, which causes the whole material to become conductive, and the critical value of this phase transition first occurs is characterized as percolation threshold.[97]

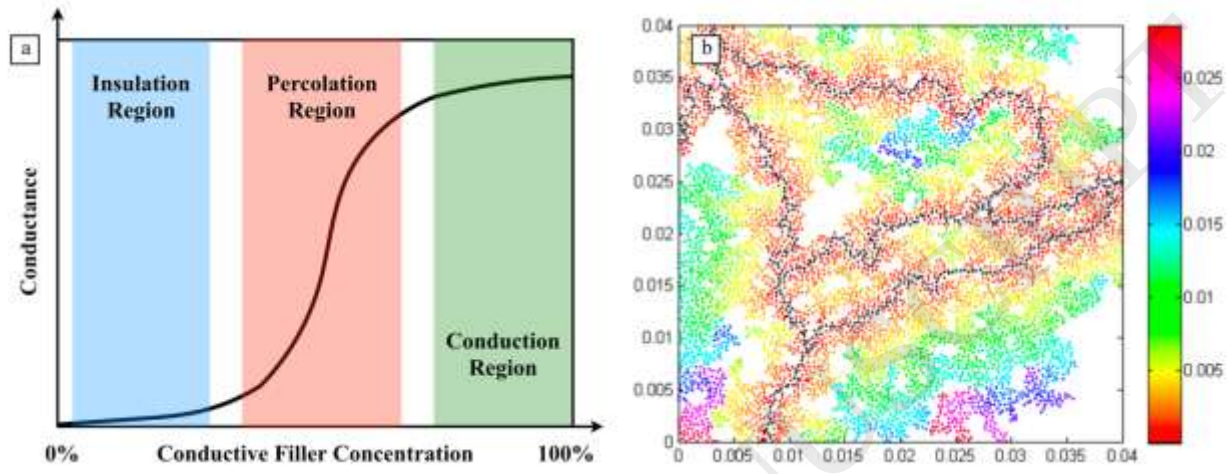

Figure 7. (a) Distance distribution of the conductive fillers in an insulting matrix. Adapted with permission from Ref. 90. (Open Access Journal). (b) Conceptual graph showing the change in conductance as a function of the concentration of conductive fillers.

To date, only few studies have employed percolation mechanism to investigate the electrical conductivity of ECHs. One example is reported by Panhuis *et al*., who revealed that the percolation threshold for CNTs in a gellan gum hydrogel was 1.3% by weight concentration, and the electrical conductivity at this point was observed to be approximately 10^{-2} S/cm.[15] In a similar study, Pekcan *et al*. used dielectric spectroscopy to investigate the percolation structure of CNTs in PAM hydrogels; and demonstrated that the electrical percolation threshold occurred at about 0.3% CNT concentration, which is consistent with the theoretical prediction.[98]

The impact of fillers on hydrogel mechanical performance can also be interpreted by the percolation theory, in which the percolation threshold is identified as the geometric phase transition.[99] Liu *et al*. investigated the potential influence of nanofiber cellulose on the mechanical properties of gelatin hydrogel.[90] As different amount of nanofiber cellulose ranged between 0 and 15 wt% were added into the hydrogel, the effects of nanofiber cellulose concentration on hydrogel performance have been found to be closely associated with percolation mechanism. The mechanical strength of the hydrogel was greatly improved as nanofiber cellulose concentration increased up to 10% by weight due to the formation of an interconnected cellulose network, suggesting the percolation threshold occurred. At a nanofiber cellulose concentration of 15 wt% and higher, more and more heterogeneous aggregation formed, resulting in a slightly decrease of hydrogel's mechanical strength.

Electrical and mechanical properties are the two most important characteristics for ECHs when applied in flexible energy storage systems, and the relationship between them in hydrogel systems is complex. Although certain phenomenological similarity exists when comparing their percolation curves, depending on the hydrogel matrix and the synthetic methods as well as the type of conductive fillers used, the electrical and mechanical percolation threshold are generally different even for a specific ECH.[100] When implementing hydrogel matrix with the conductive fillers, besides an increase of electrical conductivity, an improvement of mechanical properties can be observed. As fillers concentration keeps increasing, aggregate morphology is formed, which may lower the hydrogel viscosity and introduce defects that damage the continuity of the hydrogel network. This situation is further complicated when considering the fill-matrix interactions and self-aggregations.[87,88,91,93,95] As a result, there is an inherent tradeoff between ECHs' electrical and mechanical properties; desired nano-structure and the optimum concentration of the conductive fillers must be carefully considered based on the percolation transition.

The percolation theory offers a simple and yet detailed methodology to describe the correlation between filler concentration and certain physical properties of the composites. The experimental studies of percolation networks in ECH systems are rare even though they have been extensively applied to investigate many electrically conductive composites.[92,97] Hence, there are opportunities to explore the percolation mechanism for hydrogels infused with different types of conductive fillers, which will help to understand the chemistry of composite hydrogels at the molecular level and widen their practical applications.

4. Electrically conductive hydrogels for Flexible Supercapacitor

Supercapacitor is a key member of electrochemical energy storage system, it basically consists of two electrodes and an electrolytic medium.[36,39,101] According to the charge storage mechanism at the electrode/electrolytic phase boundaries, supercapacitor can be categorized into two distinct types: electrical double layer capacitors (EDLCs) and pseudocapacitors.[40,102] The former one involves the formation and relaxation of oppositely charged electrical layers; while the latter one requires redox reactions (intercalation or under-potential deposition) in the charge storage process.[101,103]

In order to achieve high flexibility, as well as lightweight and low cost for supercapacitors, the electroactive materials have to be coated or integrated as a thin layer onto elastic substrates, such as rubber,[104] polydimethylsiloxane,[105] paper[106] or cotton sheets;[107] these non-electroactive substrates occupy a large amount of weight and space in the final supercapacitor structure, which significantly decrease the efficiency of their overall electrochemical performances. Moreover, conventional flexible electrodes also hinder the device electrochemical performance since the effective contact between two electrodes and the middle electrolyte is limited by poor diffusion of the conventional insulated polymer gel.[101]

By contrast, ECHs combine electrical properties of metals or semiconductors with the unique properties of hydrogels, thus can sustain large mechanical deformation by themselves, offering an array of features such as high swell capacity of ionic or salt solutions, intrinsic 3D microstructured conducting network, flexibility and stretchability, providing an extremely high surface area for electrochemical reaction.[50,52] They are found to be an ideal framework to construct flexible supercapacitors.

Table 1 compares the electrochemical and mechanical characteristics of some ECHs applied in supercapacitors. As presented, the performance of a hydrogel electrode depends on the properties of electroactive materials and their interaction within the hydrogel network. Among these electroactive materials, conductive polymers,[53,108–110] graphene,[111–115] and their composites[116–123] are commonly used substances because of their high electric conductivity, large capacitance, inherent flexibility and easy to processing. The following discussion will be focused on these three types of electrode materials.

Table 1.
Electrochemical and mechanical characteristics of some electrically conducive hydrogels for flexible supercapacitor.

Electroactive Materials		Hydrogel Matrix or Gelation Agent	Specific Capacitance (F/g)	Cycling stability (cycle numbers)	Energy density (Wh/kg)	Tensile Strength (MPa)	Ref
Conductive Polymer	PANI	Polyvinyl alcohol	928 at 0.5 A/g	90% (1000)	13.6	5.3	109
	PANI	Phytic acid	480 at 0.2 A/g	83% (10000)			80
	PPy	Phytic acid	380 at 0.1 A/g	93% (2000)			51
	PANI	Polyacrylamide	315 at 2 A/g	92% (35000)			52
	PANI	H_2SO_4-polyvinyl alcohol	488 mF/cm^2 at 0.2 A/g	93% (7000)	42	0.35	110
Graphene-Based	Graphene	Hydrothermal	175 at 1 A/g		23.2	0.45	83
	Graphene	H_2SO_4-polyvinyl alcohol	186 at 1 A/g	91.6% (10000)	0.61		114

	Graphene	Hydroquinones	441 at 1 A/g	87% (10000)			113
	Graphene oxide	Ethylene Diamine	232 at 1 A/g	96% (100)		10.3	45
	N-doped graphene	Hydrothermal	113.8 at 185 A/g	95.2% (4000)	205.0		115
Composite	Graphene/Nickel	Nickel nitrate (0.04M), urea (0.2M) and NH_4F	782 at 0.2 A/g	90% (10000)			117
	PPy/Graphene	Poly (sodium 4-styrenesulfonate)	640.8 at 1 A/g	90% (2000)	35.5		120
	Graphene/Carbon/ Nanofibers	Sodium L-ascorbate	150 at 1 A/g	97.8% (2000)			112
	RuO_2/Reduced graphene oxide	Hydrothermal Method	345 at 1 A/g	100% (2000)			118
	TiO_2-Anchored Graphene	Hydrothermal Method	206.7 at 0.5 A/g	96.4% (2000)			79
	Graphene Oxide/V_2O_5	Hydrothermal Method	320 at 1.0 A/g	70% (1000)			119
	MnO_2 Decorated Graphene	Poly(dimethyl-diallyl ammonium) chloride	445.7 at 0.5 A/g	82.4% (5000)	32		121
	PPy/PEDOT/Graphene	Poly (4-styrenesulfonate)	342 at 0.5 A/g	70% (1000)	34.63		122
	CNT/PANI	Polyvinyl alcohol	315 at 0.5 A/g	92% (1500)			123

4.1 Conductive Polymer Hydrogel

The application of conductive polymer hydrogels as supercapacitors has not been realized until the pioneer work reported by Inganas *et al.*, who casted poly(3,4-ethylene-dioxythiophene)-poly(styrene sulfonate) (PEDOT-PSS) hydrogel onto a gold foil electrode.[124] CV tests revealed rectangular-shape curves even at extremely high scan rates, clearly demonstrating its capacitive characteristic. However, due to the high molecular mass of the PEDOT-PSS and water content, this world's first conductive polymer-based hydrogel electrode suffered from unsatisfied capacitance and poor mechanical strength. As a result, considerable efforts have been dedicated to developing high-performance flexible electrodes based on various CPs.

A 3D nanostructured ECH formed directly from PANI and its dopant has been demonstrated as a promising supercapacitor electrode recently.[80] The surface morphology of the dehydrated hydrogel shows the interconnected PANI nanofibers and the continuous foam-like porous nanostructured network, resulting a high conductivity of 0.11 S/cm compared with other conductive polymer hydrogels. Fig. 8a presents the CV curves of PANI hydrogel electrode, no deviation is observed even at high scan rates, indicating its fast rate-capability. Galvanostatic charge-discharge (GCD) measurements were performed at different current densities (Figure 8b), the maximum specific capacitance calculated from the discharge curves is 480 F/g at 0.2 A/g. It remains 450 F/g even when the current density increases to as high as 5 A/g (Figure 8c), which can be attributed to the effective electronic and ionic transportation within the hierarchically conductive hydrogel network. Moreover, the cycling performance of the ECH electrodes shows 93% capacitance retention after 10,000 cycles, indicating an excellent rate capability.

In addition, PPy is another conductive polymer that has been applied in the syntheses of hydrogel electrodes.[50] The electrochemical performance of PPy hydrogel was evaluated by CV and GCD measurements, in which the PPy hydrogel demonstrated a specific capacitance of 380 F/g, as well as excellent rate capability and cycle stability (Figure 8d and 8e). The structure-derived elasticity endowed PPy hydrogel electrode exceptional flexibility. Therefore, an all-solid-state supercapacitor was assembled by sandwiching a PVA-H_2SO_4 gel-like electrolyte with two pieces of PPy hydrogel electrodes, such flexible supercapacitor retained 90% capacitance after 3000 electrochemical cycles (Figure 8f). The superior electrochemical and cycle stability of PPy hydrogel can be attributed to its unique 3D conducting structure that could accommodate the swelling and shrinking of PPy polymer chain during charge-discharge processes.

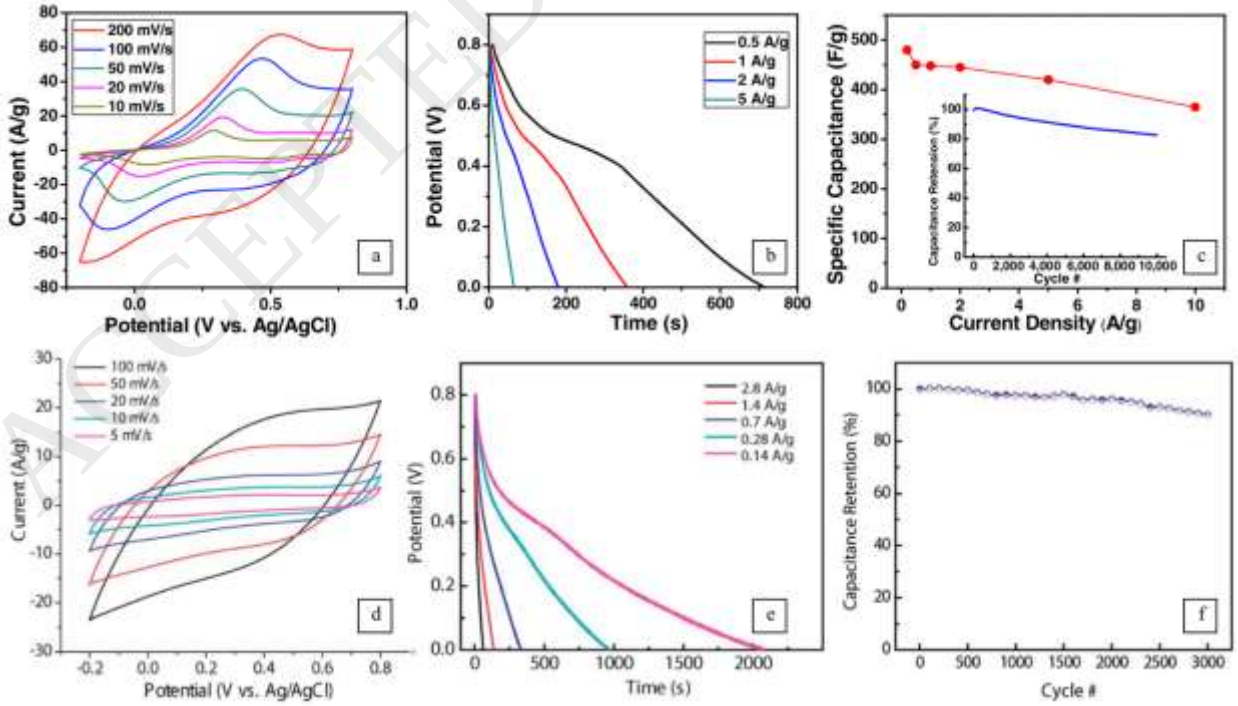

Figure 8. (a) CV curves of the PANI hydrogel electrode at different scan rates; Adapted with permission from Ref. 80. Copyright © 2012 National Academy of Sciences. (b) Specific capacitance of PPy electrodes with different material loadings at different current densities; (c) Cycling performance of PPy electrodes over 3000 charge-discharge cycles. Adapted with permission from Ref. 50. Copyright © 2014 The Royal Society of Chemistry.

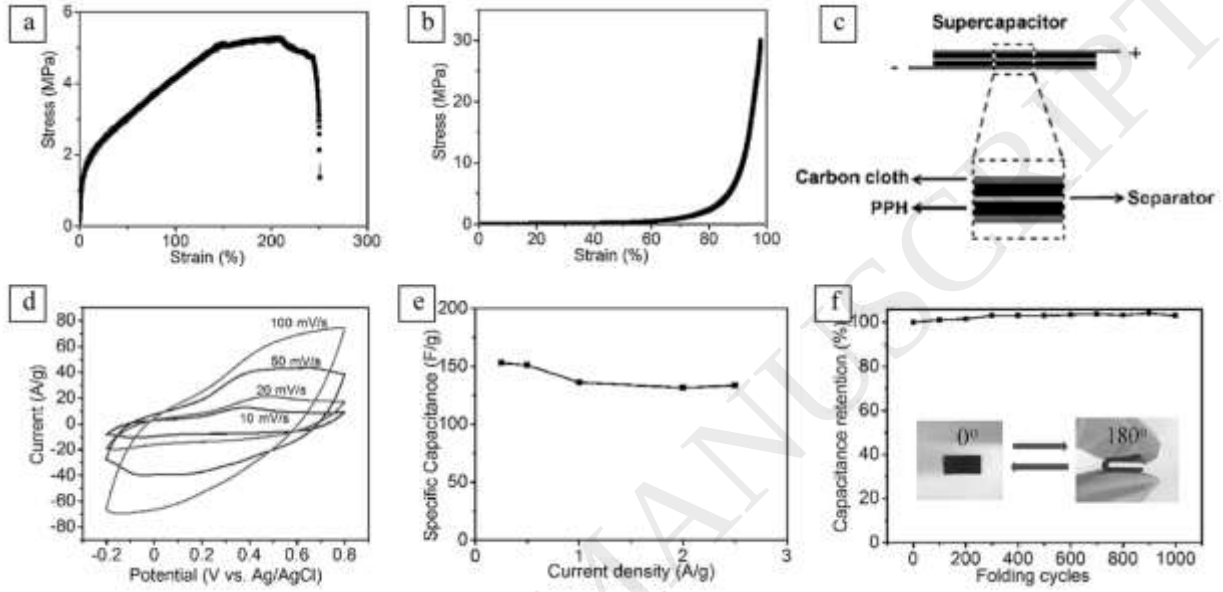

Figure 9. (a) The tensile stress-strain curve of PANI hydrogel; (b) The compression stress-stain curve of PANI hydrogel; (c) Schematic structure of a flexible solid-state supercapacitor made by PANI hydrogel electrode; (d) CV tests at scan rates of 10-100 m/V. (e) Specific capacitance of the PANI supercapacitor at varied GCD current densities; (f) Capacitance retention of the supercapacitor after 1000 mechanical folding cycles with 180 bending. Adapted with permission from Ref. 125. Copyright © 2016 WILEY-VCH Verlag GmbH & Co. KGaA, Weinheim.

A few conductive polymer hydrogels have been studied for the development of flexible supercapacitors, but most of them have shown week tensile strength and integrity. As a result, mechanically strong and electrochemically active conductive polymer hydrogels are highly desired. Ma *et al*. crosslinked a rigid conductive polymer (PANI) and a soft hydrophilic polymer (PVA) through boronic acid to form a strong and robust ECH, which mimic the dynamic structure of animal dermis.[125] As shown in Figure 9a, PANI-PVA hydrogel is mechanically robust with a tensile strength of 5.3 MPa, it can be made into a knot and stretched up to 250% (Figure 9b). Moreover, it can stand up to 98% compression and 30 MPa stress without being broken. To examine the possible application of PANI-PVA electrode for flexible supercapacitors, a symmetric solid-state supercapacitor device was fabricated based on the configuration presented in Figure 9c. The electrochemical tests showed that the solid-state supercapacitor possessed a large specific capacitance of 153 F/g and a high energy density of 13.6 Wh/kg (Figure 9d and 9e). The PANI-PVA hydrogel electrode also demonstrated excellent cycle stability, GCD tests confirmed that they could retain 90% of initial capacitance after 1000 cycles at a current density of 1 A/g (Figure 9f).

More importantly, owing to the outstanding mechanical properties, this flexible supercapacitor can retain almost 100% of its initial capacitance after 1000 cycles of 180 mechanical bending. These excellent mechanical and electrochemical properties clearly demonstrate that the PANI-PVA hydrogel-based supercapacitor is a promising power device for wearable electronics.

4.2 Graphene Hydrogel

Graphene hydrogels fabricated from hydrothermal reactions are normally mechanically strong, which can be attributed to the well-defined and interconnected 3D porous network. Figure 10a presents a scanning electron microscope (SEM) image of a typical graphene hydrogel, its pore sizes are ranged from nanometer to several micrometers, and its pore walls are made of partial overlapping or coalescing graphene sheets.[83] The compressive stress-strain curve of this graphene hydrogel is shown in Figure 10b, the elastic modulus and yield stress were measured to be 0.29 MPa and 24 kPa, respectively. Due to the π-conjugated system recovered upon the hydrothermal reduction of GO, the graphene hydrogel shows a conductivity of about 5×10^{-3} S/cm measured by the two-probe method (Figure 10c). The CV profile of the graphene hydrogel-based supercapacitor is nearly rectangular in shape (Figure 10d), indicating a good charge transport within the hydrogel electrodes. The specific capacitances is calculated to be 160 F/g at 1 A/g, which is relatively low compared with conductive polymer-based hydrogel electrodes.

To further improve the capacitive properties, hydrazine or hydroiodic acid was applied to reduce graphene hydrogels.[110] Brunauer Emmett Teller (BET) analyses indicated that chemical reduction did not affect the specific surface area of the graphene hydrogels. For electrochemical tests, reduced graphene hydrogels were directly used as the supercapacitor electrode, it exhibited a specific capacitance of 220 F/g at 1 A/g, a power density of 30 kW/kg and an energy density of 5.7 Wh/kg at a current density as high as 100 A/g (Figure 10e). The reduced graphene hydrogel electrode also demonstrated long electrical stability with ~8% capacitance loss after 2000 cycles at a current density of 4 A/g (Figure 10f).

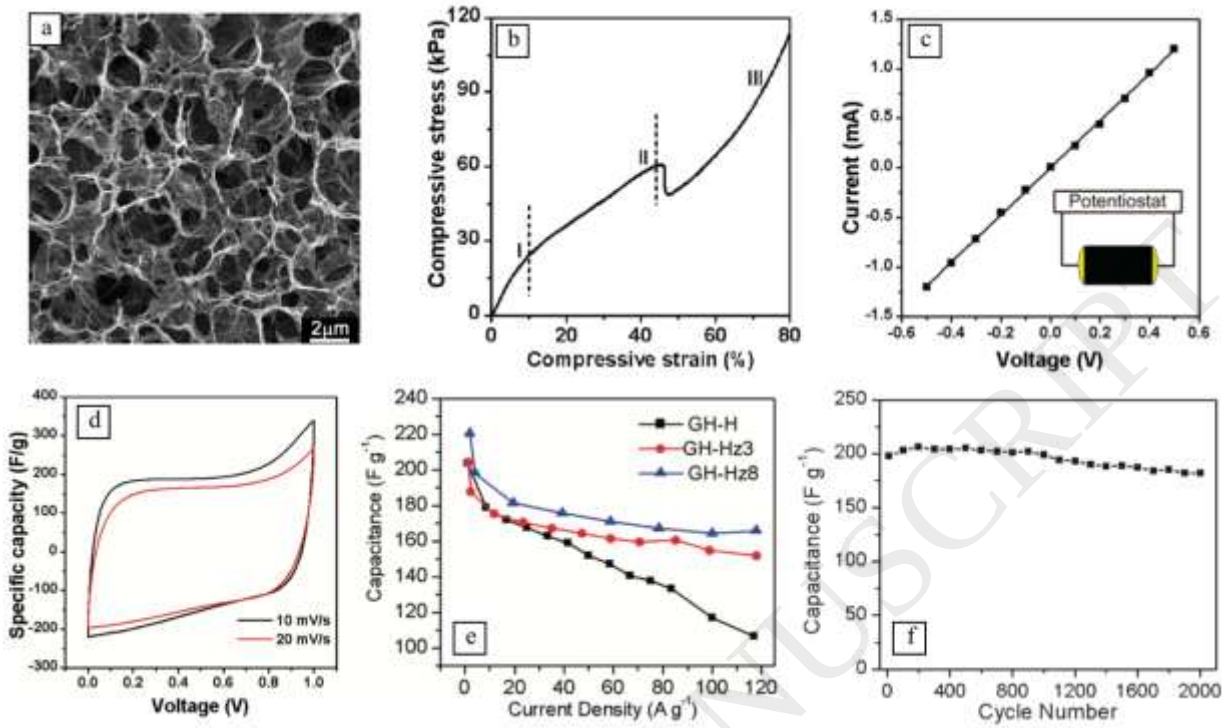

Figure 10. (a) SEM image of a typical graphene hydrogel. (b) The compressive stress-strain curve of the graphene hydrogel. (c) I-V curve of the graphene hydrogel measured by the two-probe method. (d) CV curves of the supercapacitor at different scan rates. Adapted with permission from Ref. 83. Copyright © 2010 American Chemical Society. (e) Plot of specific capacitance versus discharging current density for hydrazine reduced graphene hydrogel electrode. (f) Cycling stability of the electrode upon charging/discharging at a current density of 4 A/g. Adapted with permission from Ref. 110. Copyright © 2011 American Chemical Society.

To correlate the electrical and mechanical properties of the ECHs, Duan *et al*. fabricated a flexible solid-state supercapacitor with graphene hydrogels as the electrodes and H_2SO_4-PVA gel as the electrolyte.[113] As presented in Figure 11a, two free-standing graphene hydrogel films were first prepared by hydrothermal reduction, followed by H_2SO_4-PVA coating, then two hydrogel films were compressed together into one thin layer (Figure 11b). Due to the extensive hydrophobic and π-π interactions in the 3D network, the graphene hydrogel was strongly crosslinked and the resulting supercapacitor was highly flexible and robust. CV and galvanostatic charge/discharge tests were performed to evaluate the capacitive properties of this integrated device, which demonstrated a high gravimetric specific capacitance of 186 F/g at 1 A/g, a desirable area-specific capacitance of 372 mF/cm^2, and excellent cycling stability (8.4% capacitance decay over 10000 charge/discharge cycles at 10 A/g) (Figure 11c-11f). In addition, this supercapacitor can retain its full capacitance even under its highly bended conditions.

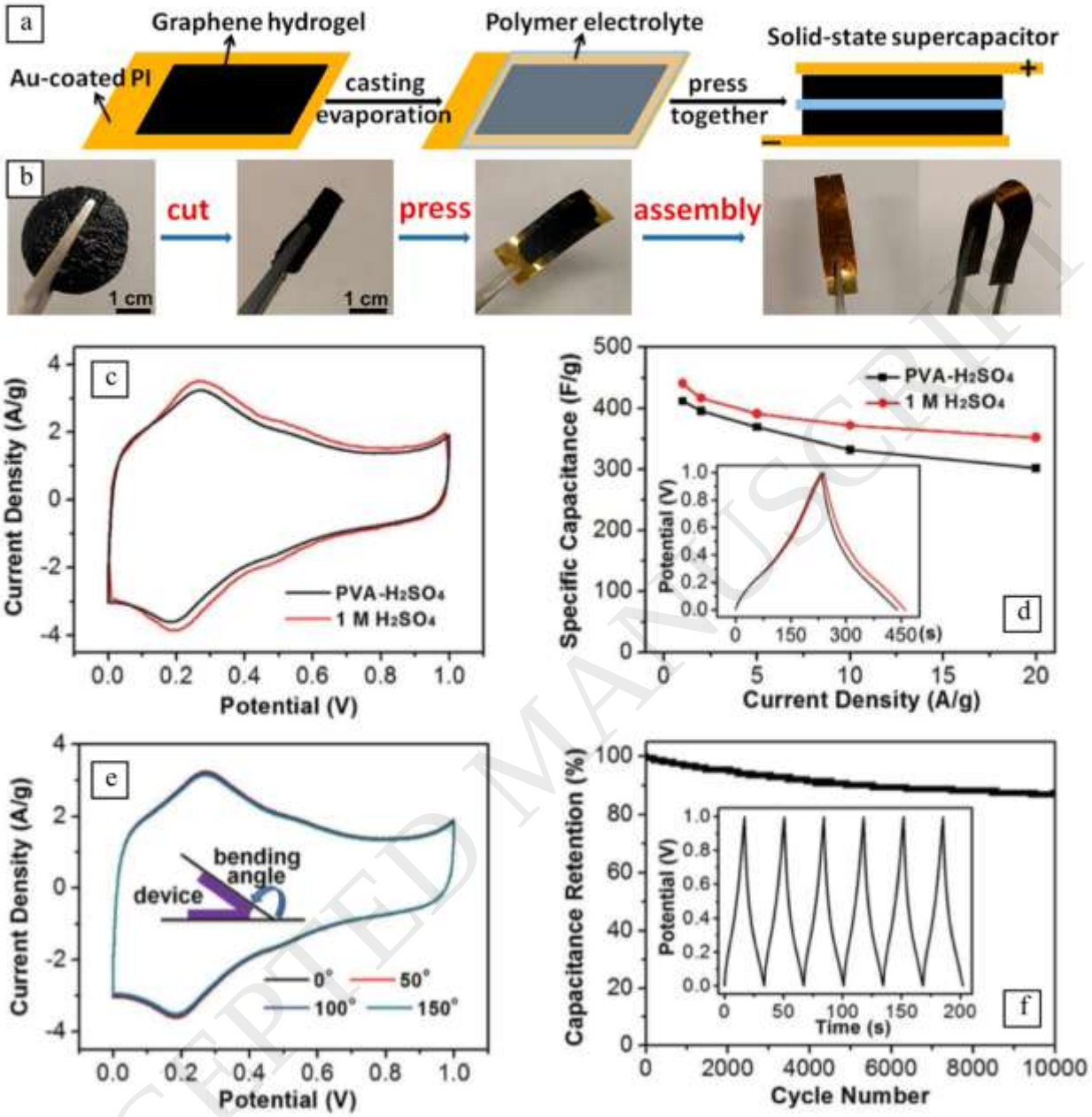

Figure 11. (a) Digital photograph of a standing graphene hydrogel electrode; (b) Schematic diagram of the solid-state flexible supercapacitor with graphene hydrogels as the electrode and H_2SO_4-PVA polymer gel as the electrolyte; (c) CV curves at 10 mV/s and (d) specific capacitances of the graphene hydrogel electrodes in H_2SO_4-PVA gel electrolyte and in 1M H_2SO_4 aqueous electrolyte; (e) CV curves of the supercapacitor at 10 mV/s with different bending angles; (d) Cycling stability of the solid-state supercapacitor under 1000 bending cycles. Adapted with permission from Ref. 113. Copyright © 2013 WILEY-VCH Verlag GmbH & Co. KGaA, Weinheim.

4.3 Composite Hydrogel

The graphene hydrogels represent a new type of materials with excellent conductivity and superior flexibility, showing great potentials in flexible energy storage applications. However, their electrochemical capacitive storage performance is far from the level of conventional

supercapacitors and the requirements of practical engineering. One of the most important reasons is that the EDLC characteristics of graphene and its derivatives are limited in ions diffusion, which is not satisfied in the capacitance property.[40,101,103] Therefore, combining graphene hydrogel with other electrical active materials to achieve optimized redox reaction and enhanced ion transportation have been designed for high-performance flexible electrodes.

Based on the considerations above, Liu *et al*. anchored spherical nanostructured TiO_2 nanoparticles onto the graphene nanosheets, developed a self-assembled three-dimensional interconnected hydrogel, which showed improved electrochemical capacitive performance.[79] The ratio of TiO_2 to graphene in the hydrogel composites can be adjusted in a wide range from 4:1 to 1:5. As depicted in Figure 12a, TiO_2 nanospheres with 20-30 nm diameters were uniformly dispersed on the graphene supports, and no aggregation were observed. Although graphene sheets tend to curve and aggregate within the hydrogel network due to the loss of surface oxygen, anchored TiO_2 nanoparticles acted as the spacer to partially prevent the aggregation, which greatly increased the specific surface area of the TiO_2 decorated graphene hydrogel. As-obtained hybrid system effectively combined electric double layer capacity of graphene with pseudocapacity of TiO_2, exhibiting a high specific capacitance of 206.7 F/g at 0.5 A/g (Figure 12b), excellent rate capability and cycling stability (Figure 12c).

Besides TiO_2, another transition metal oxide V_2O_5 has also been deposited onto graphene hydrogel to prepare high-performance hybrid electrode material.[119] Tian *et al*. developed reduced graphene oxide (rGO)/V_2O_5 composite hydrogels by a hydrothermal reaction [47] (Figure 12d). The capacitive properties of these composite hydrogels with different concentrations of V_2O_5 precursors are characterized by GCD measurements. The highest specific capacitance of about 320 F/g at a current density of 1.0 A/g is obtained (Figure 12e), and the capacitance retention ratio is over 70% after 1000 cycles (Figure 12f). The synergistic effect of combining different types of electroactive materials greatly improves the redox reaction and enhances ion transportation at the electrode/electrolyte interface. The hybrid composite electrodes are viewed as an ideal candidate for potential supercapacitor applications.

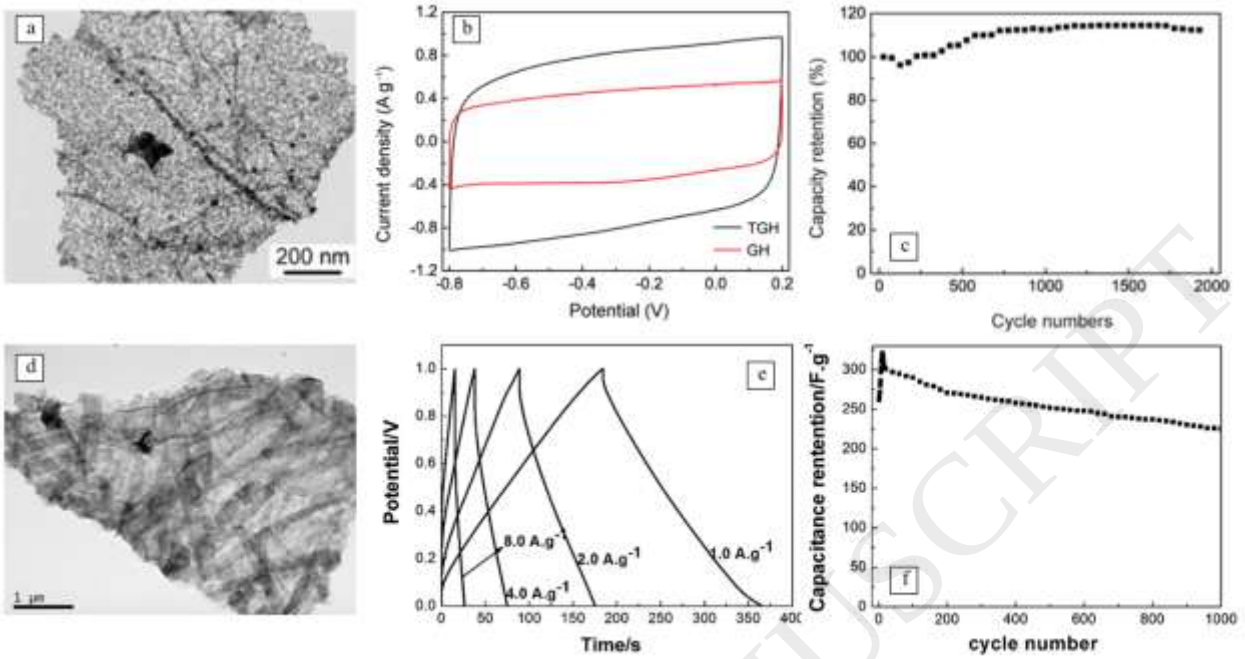

Figure 12. (a) TEM image of TiO_2 nanosphere decorated graphene hydrogel; (b) CV curves for the TiO_2 nanosphere decorated graphene hydrogel electrode and the graphene hydrogel electrode at the same scan rate of 5 mV/s; (c) Charge/discharge cycling test of the TiO_2 nanosphere decorated graphene hydrogel electrode. Adapted with permission from Ref. 79. Copyright © 2013 American Chemical Society. (d) TEM image of the rGO/V_2O_5 composite hydrogel; (e)GCD curves of the rGO/V_2O_5 hydrogel electrode measured at different current densities; (f) Cycling stability of the rGO/V_2O_5 composite hydrogel electrode at a current density of 1.0 A/g over 1000 cycles. Adapted with permission from Ref. 119. Copyright © 2014 Wiley-VCH Verlag GmbH & Co. KGaA, Weinheim.

ECHs represent a promising material for high-performance flexible supercapacitors because they could offer an enlarged electrode/electrolyte interface area for both electronic and ionic transportation, which facilitates more efficient electrochemical reactions. Besides, the inherent soft nature of hydrogels makes them ideal framework to construct flexible electrodes for wearable electronics. However, this field remains challenging since the electrochemical performances of the currently reported flexible supercapacitors are far from the level of their conventional rigid analogues, along with the poor mechanical strength and integrity of the hydrogels, significantly limit their practical applications.[36,46,126]

To overcome the problems above, great efforts and continuous innovation have been directed to explore facile and efficient fabrication methods to prepare high-performance ECHs. As a matter of fact, obtaining and processing functional hydrogels are the key steps for the development of flexible supercapacitors, with the aim of increasing electrochemical reaction and reducing the charge transport resistance at the interface, as well as improving the mechanical toleration. Furthermore, by proper functionalization, hydrogel can be equipped with additional technical features, such as self-healing, stretching and transparent, which could also be used to design functional flexible supercapacitors.

5. Electrically Conductive hydrogels for Flexible Batteries

Batteries are generally consisted of two electrochemically active electrodes separated by an ionically conductive, but electronically insulating electrolyte.[127–130] The two electrodes have different chemical potentials, when connected to an external device, electrons are forced to transfer from the negative to the positive potential, and ions are transported across the electrolyte to ensure electrical neutrality. During the same time, electrical energy are circled within the system.[44,131] The electron flow stops as long as the redox reaction at either electrode is finished. Depending on whether the batteries can be recharged, they are classified as primary and secondary batteries. Primary batteries are non-rechargeable, while secondary batteries can be recharged when a larger voltage applied in the opposite direction of the electrodes.[129,132] Lithium-ion batteries (LIBs) are the most successful secondary batteries to power an increasingly diverse range of devices, from electric vehicles to consumer electronics.[133,134]

High-performance flexible LIBs have great potential as energy sources for wearable electronics. Although tremendous efforts have been carried out, a well-developed commercialized flexible LIB has yet to be demonstrated.[41,135] One major limitation of making flexible LIB technologies a reality is to develop flexible electrodes with superior mechanical properties and reliable electrochemical performances[54]. Current technical barriers for flexible Li-ion electrodes includes: (1) conventional materials used in rigid batteries are not compatible with the flexible design; (2) inefficient ionic and electronic conductivity during operation; and (3) degradation of electrochemical performance during deformation.[57,136]

Electrically conductive hydrogels, intrinsically flexible and porous, exhibit a number of unique properties, may provide an alternative solution to solve the above-mentioned problems. To be specific, when using hydrogels in flexible LIB electrodes, they offer such advantages as compact loading of electrochemically active materials, sufficient space for volume expansion/contraction associated with the insertion of Li, continuous electronic and ionic transport pathways, and effective resistance to mechanical deformation.[55,136–138]

Researchers, over the years, have engineered hydrogels in many different ways to satisfy various requirements for flexible LIB electrodes.[139–144] Table 2 compares the electrochemical characteristics of some ECHs for flexible LIB applications. As presented, silicon (Si)-based[65,139,140,142] and transitional metal oxide-based[141,143,145] ECHs are commonly used materials for recently reported LIBs, and the following discussion will be focused on these two types of functional ECHs in view of their electrochemical and physical properties

Table 2.
Electrochemical characteristics of some electrically conducive hydrogels for flexible Li-ion battery electrode.

Electrochemical Active Nanoparticles		Electrically Conductive Fillers	Hydrogel Matrix or Gelation Agent	Capacity (mAh/g)	Cycling stability % (cycle numbers)	Coulombic Efficiency	Ref
Silicon		PANI	Phytic acid	1600 at 1 A/g	90 (5000)	70%	139
		PPy/CNTs	Phytic acid	1600 at 3.3 A/g	86 (1000)	99.5%	140
		Graphene	Hydrothermal	1020 at 4 A/g	80 (140)	53%	65
Transition metal oxides	TiO_2	PEDOT:PSS/CNTs	APS	227 at 0.5 mV/s		77.3%	143
	CuO		Chitosan	672 at 0.05 A/g	90 (500)		145
	CoO	Graphene	Hydrothermal	1025.8 at 0.1 A/g		63.7%	141

5.1 Silicon-based Hydrogels

Silicon is considered as a promising anode material for LIBs due to its high theoretical specific capacity (4200 mAh/g) and favorable working voltage.[123] Various strategies have been proposed to improve the electrochemical performance of Si-based anodes, as well as to render the electrodes flexible. For instance, Cui *et al*. implemented Si-based anodes with an ECH matrix via in-situ polymerization.[139] As shown in Figure 13a, Si nanoparticles were uniformly embedded inside the porous polymer matrix, forming intimate contact with PANI at both microscopic and molecular level. Si-PANI hydrogel was then coated on a copper foil current collector for electrochemical measurements. CV experiments of both PANI hydrogel and Si-PANI hydrogel were performed on half cells at a scan rate of 0.1 mV/s (Figure 13b). It was found that Si contribute a majority part to the capacity of the whole electrode. According to Figure 13c, at a current density of 1.0 A/g, Si-PANI composite electrode exhibits a stable capacity of 1600 mAh/g after 1,000 cycles, which is much higher than that of the electrodes made by traditional silicon binder or a simple mixture of silicon nanoparticles with PANI. The highest capacity of the composite electrode was obtained at 2,500 mAh/g with a charge/discharge rate of 0.3 A/g and 3.0 A/g. Its lithiation potential slop is between 0.3 and 0.01 V. Figure 13d and 13e demonstrate that the composite electrode can retain 91% capacity after 5000 cycles at a current density of 6 A/g, confirming its superior cycle stability.

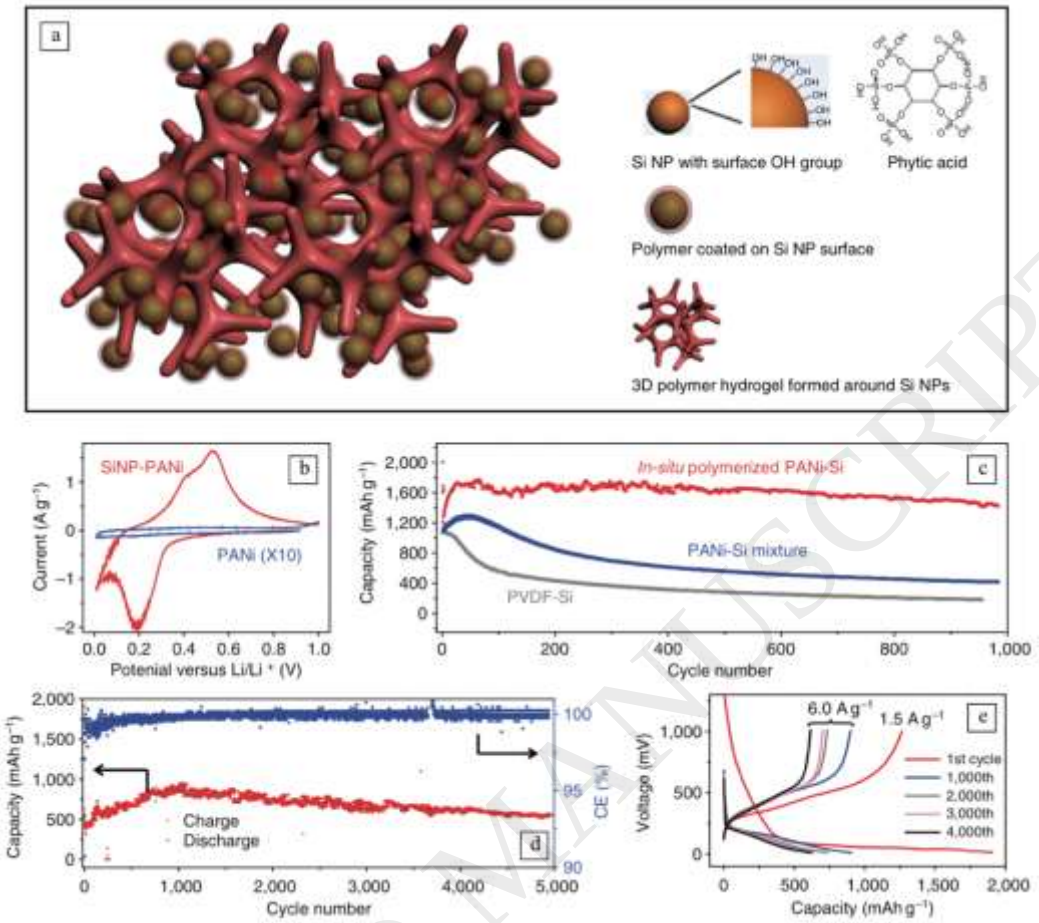

Figure 13. (a) Schematic illustration of 3D porous Si-PANI hydrogel composite; (b) CV curves of both PANI hydrogel and Si-PANI hydrogel electrodes at a scan rate of 0.1 mV/s; (c) Electrochemical cycling performance of the in-situ polymerized and simply mixed Si-PANI composite electrodes, and pure silicon electrode under charge/discharge cycles; (d) Lithiation/delithiation capacity and coulombic efficiency of Si-PANI electrode cycled at current density of 6.0 A/g for 5,000 cycles; (e) Galvanostatic charge/discharge profiles plotted for the 1st, 1000th, 2000th, 3000th and 4000th cycles. Adapted with permission from Ref. 139. Copyright © 2013 Macmillan Publishers Limited.

The Si-PANI hydrogel electrode was further extend to a ternary system by Yu *et al*., who wrapped Si nanoparticles with a 3D hierarchically ECH consisted of PPy and CNTs. [140] As shown in Figure 14a, the continuous PPy framework offering unique porous structure to facilitate the penetration of electrolyte ions and to accommodate the dramatic volume changes of Si nanoparticles. The CNTs can potentially help better disperse the Si nanoparticles in the polymer matrix and prevent aggregation (Figure 14b), thus maintaining the electron transportation throughout the entire network. Nyquist plots of the as-prepared hydrogel electrode in the frequency range of 0.1 Hz to 1 MHz were presented in Figure 14c, no obvious impedance increase was detected after the cycles, suggesting the formation of a stable solid-electrolyte-interphase. A typical CV profile of the Si/PPy/CNT electrode was shown in Figure 14d, one strong redox peak at around 0.2 V corresponded to the Si-Li alloying reaction and two well-defined redox peaks at 0.4-0.6 V associated with Si delithiation were observed. The hydrogel electrode showed the first

discharge capacity of 3600 mAh/g, which is approximately 10 times higher that of the conventional graphite anode (372 mAh/g). It was then stabilized at about 1600 mAh/g over 1000 cycles with capacity retention of 86% in a potential window of 0.01 to 1 V versus Li/Li^+ (Figure 14e). Moreover, the Coulombic efficiency for Si/PPy/CNT ternary electrode was examined to be 78.2% for the first cycle and 99.5% for the subsequent cycles (Figure 14f).

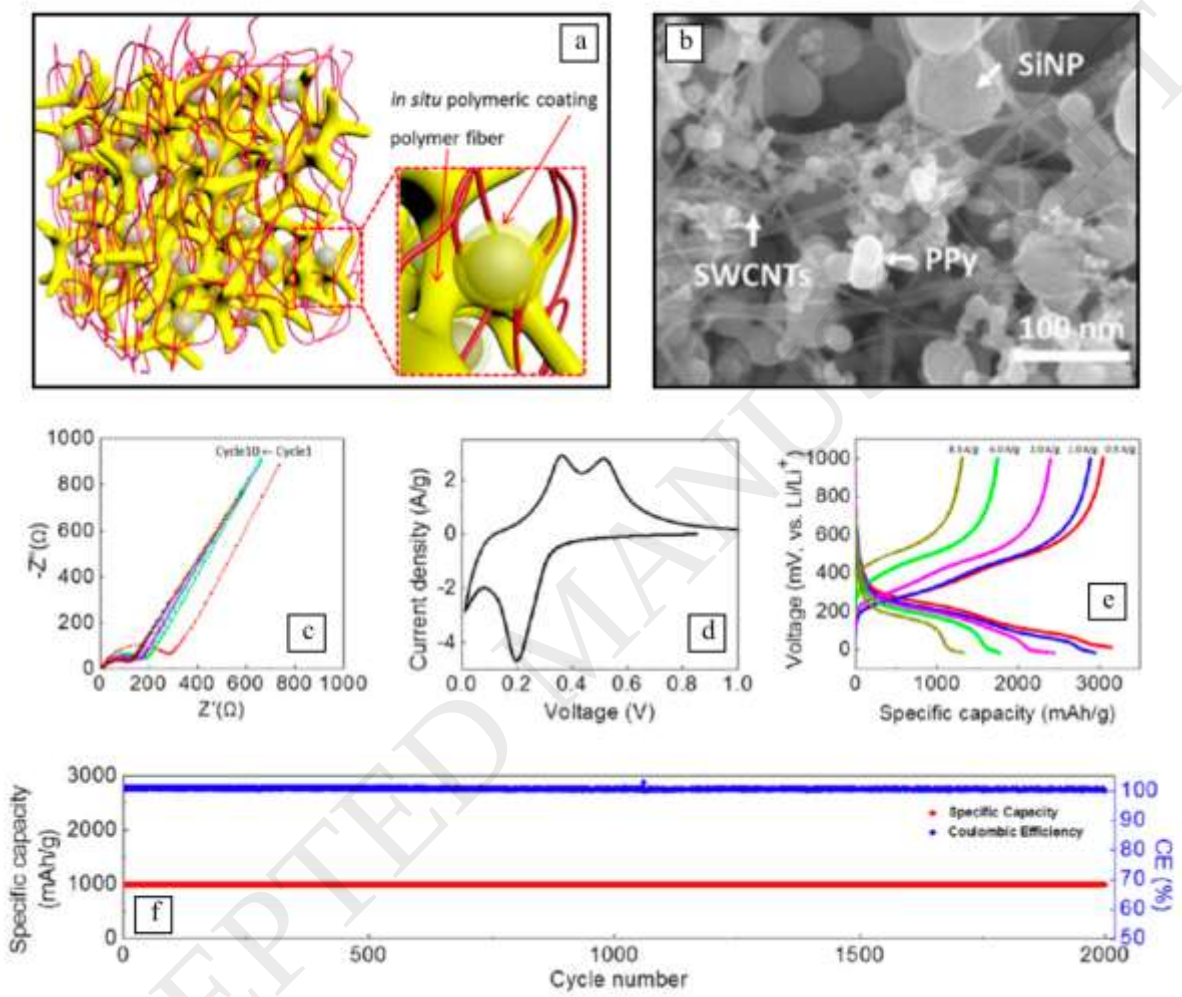

Figure 14. (a) Ternary electrode structure: Si/PPy/CNT; (b) SEM image of Si/PPy/CNT hierarchical hydrogel; (c) Nyquist plots of the hybrid electrode in the frequency range between 0.1 Hz and 1 MHz; (d) CV curve of the Si/PPy/CNT electrode at a scanning rate of 0.1 mV/s; (e) Voltage profiles of Si/PPy/CNT electrode; (f) Discharge capacity and Coulombic efficiency of the Si/PPy/CNT electrode. Adapted with permission from Ref. 140. Copyright © 2013 American Chemical Society.

Apart from wrapping Si nanoparticles with CPs, anchoring Si nanoparticles on the surface of graphene sheets is another efficient way to boost their electrochemical performance when acting as LIB electrodes. Jiang *et al*. prepared a porous graphene hydrogel coated with Si nanoparticles via a solution-based self-assembly process.[65] An ultrathin SiO_X layer was fabricated on the surface of the Si nanoparticles to improve their dispersion in the matrix and enhance their interfacial adhesion with graphene sheet. LIB Electrodes constructed from Si-graphene hydrogel

exhibited a stable storage capacity of 1020 mAh/g at 4 A/g and long cyclic stability (1640 mAh/g after 140 cycles at 0.1 A/g). By taking advantage of the continuous-conducting network of ECHs, Si nanoparticles can be uniformly distributed and electronically connected, resulting a well-connected flexible LIB electrode with excellent electrochemical performance.

5.2 Transitional Metal Oxide-Based Hydrogels

Nanostructured transition metal oxides are another type of promising LIB electrode material due to their high electrical conductivity and theoretical capacity, and moderate voltage window for safe Li storage.[41,132] Recently, Bao *et al*. built a hybrid hydrogel system based on carbon nanotube and conductive polymer network, which further loaded with TiO_2 nanoparticles to improve its capacity for advanced LIB electrodes.[143] The fabrication procedure is illustrated in Figure 15a. A homogenous solution containing water-stable PEDOT:PSS, well-dispersed CNT and TiO_2 nanoparticles was prepared at first, then adding gelation agents to form a hydrogel, which can be peeled off as a freestanding film and cut into different sizes and shapes for cell assemble. The hydrogel was polymerized in-situ, resulting in an interconnected 3D architecture, where CNT was essential to ensure mechanical robustness and flexibility, PEDOT:PSS was responsible for efficient transport of de-localized electrons to obtain high conductivity; and TiO_2 was chosen to achieve high capacity and electrochemical stability. When TiO_2 nanoparticles were incorporated into PEDOT:PSS/CNT hydrogel, a representative composition of 57%-TiO_2, 28%-CNT and 15%-polymer (by weight) was used for investigation. As shown in Figure 15b, CNT penetrates through the whole structure, while TiO_2 nanoparticles form clusters embedded within the matrix. This robust network provides TiO_2-PEDOT:PSS-CNT electrode superior electrical properties even after 500 repeated bending cycles with a bending radius of 3.5 mm. Compared with the TiO_2 electrode made from poly(vinylidene fluoride) (PVDF) binder, TiO_2-PEDOT:PSS-CNT electrode shows a much higher charge storage capacity of 76 mAh/g in 4000s of charge/discharge. Moreover, the TiO_2-loaded hydrogel system demonstrates a high areal capacity of 2.2 mAh/cm^2 at 0.1C rate (Figure 15c & 15d). By coupling desirable anode or cathode active materials with this hybrid CNT-conductive polymer hydrogel system, flexible batteries with reliable mechanical properties can be facilely fabricated.

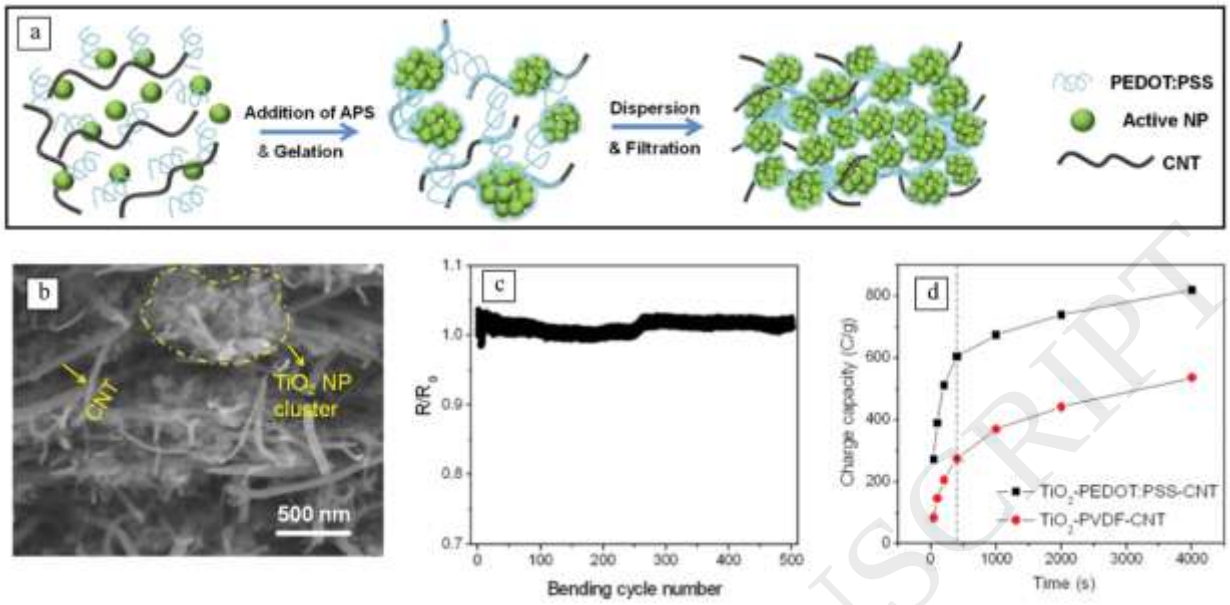

Figure 15. (a) Schematic illustration of the aqueous solution process to fabricate PEDOT:PSS/CNT flexible electrodes; (b) SEM image of the TiO_2-PEDOT:PSS-CNT film electrode; (c) Resistance of the TiO_2-PEDOT:PSS-CNT electrode over 500 bending cycles with a bending radius of 3.5 mm; (d) Capacity dependence of each electrode versus charging time. Adapted with permission from Ref. 143. Copyright © 2014 WILEY-VCH Verlag GmbH & Co. KGaA, Weinheim.

To better accommodate the large volume expansion caused by the insertion of Li, electrochemical active nanoparticles with a large interior void space was proposed to fabricate LIB electrodes. Lu *et al*. developed a supramolecular hydrogel crosslinked of hollowed CuO and chitosan.[145] Such hydrogel electrode demonstrated a competitive stable discharge capacity of 430 mAh/g and a retention of 90% after 500 cycles. CoO is another transition metal oxide that have been applied for the preparation of LIB electrodes,[141] Jia *et al*. anchored CoO nanoparticles on the graphene surface to form a 3D CoO-graphene hydrogel electrode. It delivers high specific capacity of 1025.8mAh/g at 100 mA/g, indicating its outstanding rate capability.

LIB electrodes fabricated from ECHs possess a more complicated architecture by incorporating a variety of active materials, leading to a more complicated structure with unique features compared with traditional electrodes. These include: (1) the porous hydrogel scaffold provides large interior space for dramatic volume change of electrochemical active nanoparticles; (2) a continuous-conducting network promotes efficient and rapid pathways for electron and ion transfer; and (3) the interconnected and entangled polymer matrix ensures excellent mechanical robustness. The fabrication of hybrid ECHs that combine the advantages of each component have allowed us to develop next-generation flexible LIBs with improved mechanical and electrochemical properties.

6. Conclusions and Outlook

This review compiles the state-of-the-art and the progress in hydrogel materials for flexible energy storage applications, with a focus on supercapacitors and batteries. From the viewpoint of material design, the conductive, soft and mechanically robust ECHs are the ideal platform to construct flexible electronic devices. As a matter of fact, obtaining and processing hydrogel materials with desired properties are the key steps for the fabrication of flexible energy storage systems from start to finish, many strategies have been developed to reach such steps. Specifically, one interesting approach is to combine conductive polymers or graphene with the hydrogel electrodes to improve energy storage and power density performances; similarly, mixing transition metal oxide with the hydrogel electrolytes represents an attractive method to achieve superior cycling stability; increasing surface area, porosity and developing well-connected channels within the hydrogel structure that favor electron transfer and ion diffusion are also promising pathways to enhance the electrochemical performance of supercapacitors and batteries.

In spite of the achievements discussed in this review, the development of ECH in flexible energy storage systems is still in the early stages. There remain substantial scientific and technological challenges for the fabrication of high performance ECHs before bringing them towards the practical applications:

(1) As described in the percolation theory, although a large number of electro-active materials can be integrated with hydrogels to fabricate flexible supercapacitors and batteries, an optimized composition of the electro-active materials and the hydrogel matrix is always required to balance its mechanical and electrochemical properties. Therefore, highly flexible energy storage systems with superior energy/power densities and excellent cyclic stability are still mostly desired.

(2) Flexibility is an important criterion for the selection of hydrogel materials in wearable electronic applications. However, there are no accurate evaluation methods to precisely measure flexibility. Although bending test and stretching test have been commonly used to characterize the mechanical properties of hydrogels, the standards or metrologies for the experimental setup and the assessment of electrochemical performance with respect to the bending behaviors (bending angles, times, or radius) of the devices, are still need to be established.

(3) The search for new hydrogel materials with excellent electrochemical and mechanical performance is only the first step towards the development of flexible energy storage devices, which also requires a reliable configuration and structural design to integrate all components into a single unit and then assemble into the final products. At present, applying these flexible energy storage devices to power everyday electronics is still limited in the laboratories.

(4) As future technological innovations gear toward miniaturizing electronics and maximizing performance, there is an increasing demand to extend the scope of the current systems to fabricate lightweight and thin hydrogel materials for flexible micro-supercapacitors and micro-batteries. Meanwhile, miniaturized electronic devices with multiple functionalities such as optical transparency, biocompatibility and self-healing, will be the major challenges facing further development of flexible energy storage devices.

Fortunately, electronics industry has also recognized the need to push new advances in flexible energy storage technology. During the last decade, this field has witnessed a dramatic expansion of patent applications and literature publications, which demonstrating the tremendous efforts of worldwide commercial companies to bring flexible energy storage devices towards the daily usage. With the intense research from both academia and industry, we envision that the breakthrough of flexible energy storage technology will take place soon.

Acknowledgment

The work was supported by NSFC (grant number: 11472080 and 51731004), NSF of Jiangsu Province (grant number: BK20141336), Fundamental Research Funds for the Central Universities and NSERC (grant number: RGPIN-2014-04663).

References

[1] Sangeetha NM, Maitra U. Supramolecular gels: Functions and uses. Chem Soc Rev 2005;34:821. doi:10.1039/b417081b.

[2] Johnson JA, Turro NJ, Koberstein JT, Mark JE. Some hydrogels having novel molecular structures. Prog Polym Sci 2010;35:332–7. doi:10.1016/j.progpolymsci.2009.12.002.

[3] Guiseppi-Elie A. Electroconductive hydrogels: Synthesis, characterization and biomedical applications. Biomaterials 2010;31:2701–16. doi:10.1016/j.biomaterials.2009.12.052.

[4] Zhao F, Shi Y, Pan L, Yu G. Multifunctional Nanostructured Conductive Polymer Gels: Synthesis, Properties, and Applications. Acc Chem Res 2017;50:1734–43. doi:10.1021/acs.accounts.7b00191.

[5] Estroff LA, Hamilton AD. Water gelation by small organic molecules. Chem Rev 2004;104:1201–17. doi:10.1021/cr0302049.

[6] Jeong B, Wan S, Han Y. Thermosensitive sol – gel reversible hydrogels. Adv Drug Deliv Rev 2002;54:37–51. doi:10.1016/j.addr.2012.09.012.

[7] Sahiner N. Soft and flexible hydrogel templates of different sizes and various functionalities for metal nanoparticle preparation and their use in catalysis. Prog Polym Sci 2013;38:1329–56. doi:10.1016/j.progpolymsci.2013.06.004.

[8] Peppas NA, Bures P, Leobandung W, Ichikawa H. Hydrogels in pharmaceutical formulations. Eur J Pharm Biopharm 2000;50:27–46. doi:10.1016/S0939-6411(00)00090-4.

[9] Asher SA, Holtz JH. Polymerized colloidal crystal hydrogel film as intelligent chemical sensing materials. Nature 1997;389:829–32. doi:10.1038/39834.

[10] Wang W, Zhang Y, Liu W. Bioinspired fabrication of high strength hydrogels from non-covalent interactions. Prog Polym Sci 2017;71:1–25. doi:10.1016/j.progpolymsci.2017.04.001.

[11] Shapiro YE. Structure and dynamics of hydrogels and organogels: An NMR spectroscopy approach. Prog Polym Sci 2011;36:1184–253. doi:10.1016/j.progpolymsci.2011.04.002.

[12] Shi Z, Gao X, Ullah MW, Li S, Wang Q, Yang G. Electroconductive natural polymer-based hydrogels. Biomaterials 2016;111:40–54. doi:10.1016/j.biomaterials.2016.09.020.

[13] Sekine S, Ido Y, Miyake T, Nagamine K, Nishizawa M. Conducting polymer electrodes printed on hydrogel. J Am Chem Soc 2010;132:13174–5. doi:10.1021/ja1062357.

[14] You JO, Auguste DT. Conductive, physiologically responsive hydrogels. Langmuir 2010;26:4607–12. doi:10.1021/la100294p.

[15] Ferris CJ, in het Panhuis M. Conducting bio-materials based on gellan gum hydrogels. Soft Matter 2009;5:3430. doi:10.1039/b909795c.

[16] Liao M, Wan P, Wen J, Gong M, Wu X, Wang Y, et al. Wearable, Healable, and Adhesive Epidermal Sensors Assembled from Mussel-Inspired Conductive Hybrid Hydrogel Framework. Adv Funct Mater 2017;27:1–11. doi:10.1002/adfm.201703852.

[17] Zhou H, Yao W, Li G, Wang J, Lu Y. Graphene/poly(3,4-ethylenedioxythiophene) hydrogel with excellent mechanical performance and high conductivity. Carbon N Y 2013;59:495–502. doi:10.1016/j.carbon.2013.03.045.

[18] Han L, Lu X, Liu K, Wang K, Fang L, Weng L-T, et al. Mussel-Inspired Adhesive and Tough Hydrogel Based on Nanoclay Confined Dopamine Polymerization. ACS Nano 2017;11:2561–74. doi:10.1021/acsnano.6b05318.

[19] Cong HP, Wang P, Yu SH. Stretchable and self-healing graphene oxide-polymer composite hydrogels: A dual-network design. Chem Mater 2013;25:3357–62.

doi:10.1021/cm401919c.
[20] Chortos A, Bao Z. Skin-inspired electronic devices. Mater Today 2014;17:321–31. doi:10.1016/j.mattod.2014.05.006.
[21] Dong L, Xu C, Li Y, Huang Z-H, Kang F, Yang Q-H, et al. Flexible electrodes and supercapacitors for wearable energy storage: a review by category. J Mater Chem A 2016;4:4659–85. doi:10.1039/C5TA10582J.
[22] Liu W, Song M-S, Kong B, Cui Y. Flexible and Stretchable Energy Storage: Recent Advances and Future Perspectives. Adv Mater 2017;29:1603436. doi:10.1002/adma.201603436.
[23] Bai H, Li C, Wang X, Shi G. A pH-sensitive graphene oxide composite hydrogel. Chem Commun 2010;46:2376. doi:10.1039/c000051e.
[24] Cui Z, Zhou M, Greensmith PJ, Wang W, Hoyland JA, Kinloch IA, et al. A study of conductive hydrogel composites of pH-responsive microgels and carbon nanotubes. Soft Matter 2016;12:4142–53. doi:10.1039/C6SM00223D.
[25] Jiang X, Xiang N, Wang J, Zhao Y, Hou L. Preparation and characterization of hybrid double network chitosan/poly(acrylic amide-acrylic acid) high toughness hydrogel through Al3+crosslinking. Carbohydr Polym 2017;173:701–6. doi:10.1016/j.carbpol.2017.06.003.
[26] Guo B, Glavas L, Albertsson AC. Biodegradable and electrically conducting polymers for biomedical applications. Prog Polym Sci 2013;38:1263–86. doi:10.1016/j.progpolymsci.2013.06.003.
[27] Guarino V, Alvarez-Perez MA, Borriello A, Napolitano T, Ambrosio L. Conductive PANi/PEGDA Macroporous Hydrogels For Nerve Regeneration. Adv Healthc Mater 2013;2:218–27. doi:10.1002/adhm.201200152.
[28] Ding H, Zhong M, Kim YJ, Pholpabu P, Balasubramanian A, Hui CM, et al. Biologically Derived Soft Conducting Hydrogels Using Heparin-Doped Polymer Networks. ACS Nano 2014;8:4348–57. doi:10.1021/nn406019m.
[29] Szunerits S, Teodorescu F, Boukherroub R. Electrochemically triggered release of drugs. Eur Polym J 2016;83:467–77. doi:10.1016/j.eurpolymj.2016.03.001.
[30] Yang JA, Yeom J, Hwang BW, Hoffman AS, Hahn SK. In situ-forming injectable hydrogels for regenerative medicine. Prog Polym Sci 2014;39:1973–86. doi:10.1016/j.progpolymsci.2014.07.006.
[31] Hoare TR, Kohane DS. Hydrogels in drug delivery: Progress and challenges. Polymer (Guildf) 2008;49:1993–2007. doi:10.1016/j.polymer.2008.01.027.
[32] Hur J, Im K, Kim SW, Kim J, Chung DY, Kim TH, et al. Polypyrrole/agarose-based electronically conductive and reversibly restorable hydrogel. ACS Nano 2014;8:10066–76. doi:10.1021/nn502704g.
[33] Alam A, Zhang Y, Kuan H-C, Lee S-H, Ma J. Polymer composite hydrogels containing carbon nanomaterials—Morphology and mechanical and functional performance. Prog Polym Sci 2018;77:1–18. doi:10.1016/j.progpolymsci.2017.09.001.
[34] Meng Y, Zhao Y, Hu C, Cheng H, Hu Y, Zhang Z, et al. All-graphene core-sheath microfibers for all-solid-state, stretchable fibriform supercapacitors and wearable electronic textiles. Adv Mater 2013;25:2326–31. doi:10.1002/adma.201300132.
[35] Tai Y, Mulle M, Aguilar Ventura I, Lubineau G. A highly sensitive, low-cost, wearable pressure sensor based on conductive hydrogel spheres. Nanoscale 2015;7:14766–73. doi:10.1039/C5NR03155A.

[36] Wang G, Zhang L, Zhang J. A review of electrode materials for electrochemical supercapacitors. Chem Soc Rev 2012;41:797–828. doi:10.1039/C1CS15060J.
[37] Salanne M, Rotenberg B, Naoi K, Kaneko K, Taberna P-L, Grey CP, et al. Efficient storage mechanisms for building better supercapacitors. Nat Energy 2016;1:16070. doi:10.1038/nenergy.2016.70.
[38] Winter M, Brodd RJ. What Are Batteries, Fuel Cells, and Supercapacitors? Chem Rev 2004;104:4245–70. doi:10.1021/cr020730k.
[39] Wang Y, Song Y, Xia Y. Electrochemical capacitors: mechanism, materials, systems, characterization and applications. Chem Soc Rev 2016;45:5925–50. doi:10.1039/C5CS00580A.
[40] Chee WK, Lim HN, Zainal Z, Huang NM, Harrison I, Andou Y. Flexible Graphene-Based Supercapacitors: A Review. J Phys Chem C 2016;120:4153–72. doi:10.1021/acs.jpcc.5b10187.
[41] Bruce PG, Scrosati B, Tarascon JM. Nanomaterials for rechargeable lithium batteries. Angew Chemie - Int Ed 2008;47:2930–46. doi:10.1002/anie.200702505.
[42] Armand M, Tarascon JM. Building better batteries. Nature 2008;451:652–7. doi:10.1038/451652a.
[43] Tarascon JM, Armand M. Issues and challenges facing rechargeable lithium batteries. Nature 2001;414:359–67. doi:10.1038/35104644.
[44] Whittingham MS. Lithium batteries and cathode materials. Chem Rev 2004;104:4271–301. doi:10.1021/cr020731c.
[45] Luan VH, Tien HN, Hoa LT, Hien NTM, Oh E-S, Chung J, et al. Synthesis of a highly conductive and large surface area graphene oxide hydrogel and its use in a supercapacitor. J Mater Chem A 2013;1:208–11. doi:10.1039/C2TA00444E.
[46] Choudhury NA, Sampath S, Shukla AK. Hydrogel-polymer electrolytes for electrochemical capacitors: an overview. Energy Environ Sci 2009;2:55–67. doi:10.1039/B811217G.
[47] Wu X-L, Xu A-W. Carbonaceous hydrogels and aerogels for supercapacitors. J Mater Chem A 2014;2:4852–64. doi:10.1039/C3TA13929H.
[48] Shi Y, Peng L, Yu G. Nanostructured conducting polymer hydrogels for energy storage applications. Nanoscale 2015;7:12796–806. doi:10.1039/C5NR03403E.
[49] Guo H, He W, Lu Y, Zhang X. Self-crosslinked polyaniline hydrogel electrodes for electrochemical energy storage. Carbon N Y 2015;92:133–41. doi:10.1016/j.carbon.2015.03.062.
[50] Shi Y, Pan L, Liu B, Wang Y, Cui Y, Bao Z, et al. Nanostructured conductive polypyrrole hydrogels as high-performance, flexible supercapacitor electrodes. J Mater Chem A 2014;2:6086–91. doi:10.1039/C4TA00484A.
[51] Hao GP, Hippauf F, Oschatz M, Wisser FM, Leifert A, Nickel W, et al. Stretchable and semitransparent conductive hybrid hydrogels for flexible supercapacitors. ACS Nano 2014;8:7138–46. doi:10.1021/nn502065u.
[52] Armelin E, Pérez-Madrigal MM, Alemán C, Díaz DD. Current status and challenges of biohydrogels for applications as supercapacitors and secondary batteries. J Mater Chem A 2016;4:8952–68. doi:10.1039/C6TA01846G.
[53] Shown I, Ganguly A, Chen LC, Chen KH. Conducting polymer-based flexible supercapacitor. Energy Sci Eng 2015;3:1–25. doi:10.1002/ese3.50.
[54] Hu Y, Sun X. Flexible rechargeable lithium ion batteries: advances and challenges in

materials and process technologies. J Mater Chem A 2014;2:10712–38. doi:10.1039/C4TA00716F.
[55] Liu QC, Xu JJ, Xu D, Zhang XB. Flexible lithium-oxygen battery based on a recoverable cathode. Nat Commun 2015;6:1–8. doi:10.1038/ncomms8892.
[56] Zhang Y, Bai W, Cheng X, Ren J, Weng W, Chen P, et al. Flexible and stretchable lithium-ion batteries and supercapacitors based on electrically conducting carbon nanotube fiber springs. Angew Chemie - Int Ed 2014;53:14564–8. doi:10.1002/anie.201409366.
[57] Gwon H, Hong J, Kim H, Seo D-H, Jeon S, Kang K. Recent progress on flexible lithium rechargeable batteries. Energy Environ Sci 2014;7:538–51. doi:10.1039/C3EE42927J.
[58] Javadi M, Gu Q, Naficy S, Farajikhah S, Crook JM, Wallace GG, et al. Conductive Tough Hydrogel for Bioapplications. Macromol Biosci 2018;18:1–11. doi:10.1002/mabi.201700270.
[59] Kishi R, Hiroki K, Tominaga T, Sano KI, Okuzaki H, Martinez JG, et al. Electro-conductive double-network hydrogels. J Polym Sci Part B Polym Phys 2012;50:790–6. doi:10.1002/polb.23066.
[60] Yao B, Wang H, Zhou Q, Wu M, Zhang M, Li C, et al. Ultrahigh-Conductivity Polymer Hydrogels with Arbitrary Structures. Adv Mater 2017;29:1–7. doi:10.1002/adma.201700974.
[61] Shen J, Yan B, Li T, Long Y, Li N, Ye M. Mechanical, thermal and swelling properties of poly(acrylic acid)–graphene oxide composite hydrogels. Soft Matter 2012;8:1831–6. doi:10.1039/C1SM06970E.
[62] Gao H, Sun Y, Zhou J, Xu R, Duan H. Mussel-inspired synthesis of polydopamine-functionalized graphene hydrogel as reusable adsorbents for water purification. ACS Appl Mater Interfaces 2013;5:425–32. doi:10.1021/am302500v.
[63] Ahn Y, Lee H, Lee D, Lee Y. Highly conductive and flexible silver nanowire-based microelectrodes on biocompatible hydrogel. ACS Appl Mater Interfaces 2014;6:18401–7. doi:10.1021/am504462f.
[64] Kim G-P, Sun H-H, Manthiram A. Design of a sectionalized MnO 2 -Co 3 O 4 electrode via selective electrodeposition of metal ions in hydrogel for enhanced electrocatalytic activity in metal-air batteries. Nano Energy 2016;30:130–7. doi:10.1016/j.nanoen.2016.10.003.
[65] Bai X, Yu Y, Kung HH, Wang B, Jiang J. Si@SiOx/graphene hydrogel composite anode for lithium-ion battery. J Power Sources 2016;306:42–8. doi:10.1016/j.jpowsour.2015.11.102.
[66] Jiang J, Huang Y, Wang Y, Xu H, Xing M, Zhong W. Mussel-Inspired Dopamine and Carbon Nanotube Leading to a Biocompatible Self-Rolling Conductive Hydrogel Film. Materials (Basel) 2017;10:964. doi:10.3390/ma10080964.
[67] Wu Y, Chen YX, Yan J, Yang S, Dong P, Soman P. Fabrication of conductive polyaniline hydrogel using porogen leaching and projection microstereolithography. J Mater Chem B 2015;3:5352–60. doi:10.1039/C5TB00629E.
[68] Zhao D, Zhang Q, Chen W, Yi X, Liu S, Wang Q, et al. Highly Flexible and Conductive Cellulose-Mediated PEDOT:PSS/MWCNT Composite Films for Supercapacitor Electrodes. ACS Appl Mater Interfaces 2017;9:13213–22. doi:10.1021/acsami.7b01852.
[69] Hu K, Kulkarni DD, Choi I, Tsukruk V V. Graphene-polymer nanocomposites for structural and functional applications. Prog Polym Sci 2014;39:1934–72.

doi:10.1016/j.progpolymsci.2014.03.001.
[70] Dreyer DR, Park S, Bielawski CW, Ruoff RS. Graphite oxide. Chem Soc Rev 2010;39:228–40. doi:10.1039/b917103g.
[71] De Volder MFL, Tawfick SH, Baughman RH, Hart AJ. Carbon Nanotubes: Present and Future Commercial Applications. Science (80-) 2013;339:535–9. doi:10.1126/science.1222453.
[72] Alzari V, Nuvoli D, Scognamillo S, Piccinini M, Gioffredi E, Malucelli G, et al. Graphene-containing thermoresponsive nanocomposite hydrogels of poly(N-isopropylacrylamide) prepared by frontal polymerization. J Mater Chem 2011;21:8727. doi:10.1039/c1jm11076d.
[73] Han L, Lu X, Wang M, Gan D, Deng W, Wang K, et al. A Mussel-Inspired Conductive, Self-Adhesive, and Self-Healable Tough Hydrogel as Cell Stimulators and Implantable Bioelectronics. Small 2017;13:1601916. doi:10.1002/smll.201601916.
[74] Li X, Yang Q, Zhao Y, Long S, Zheng J. Dual physically crosslinked double network hydrogels with high toughness and self-healing properties. Soft Matter 2017;13:911–20. doi:10.1039/C6SM02567F.
[75] Nakayama A, Kakugo A, Gong JP, Osada Y, Takai M, Erata T, et al. High mechanical strength double-network hydrogel with bacterial cellulose. Adv Funct Mater 2004;14:1124–8. doi:10.1002/adfm.200305197.
[76] Pissis P, Kyritsis A. Electrical conductivity studies in hydrogels. Solid State Ionics 1997;97:105–13. doi:Doi 10.1016/S0167-2738(97)00074-X.
[77] Brahim S, Guiseppi-Elie A. Electroconductive hydrogels: Electrical and electrochemical properties of polypyrrole-poly(HEMA) composites. Electroanalysis 2005;17:556–70. doi:10.1002/elan.200403109.
[78] Runge MB, Dadsetan M, Baltrusaitis J, Ruesink T, Lu L, Windebank AJ, et al. Development of electrically conductive oligo(polyethylene glycol) fumarate-polypyrrole hydrogels for nerve regeneration. Biomacromolecules 2010;11:2845–53. doi:10.1021/bm100526a.
[79] Zhang Z, Xiao F, Guo Y, Wang S, Liu Y. One-Pot Self-Assembled Three-Dimensional TiO 2 -Graphene Hydrogel with Improved Adsorption Capacities and Photocatalytic and Electrochemical Activities. ACS Appl Mater Interfaces 2013;5:2227–33. doi:10.1021/am303299r.
[80] Pan L, Yu G, Zhai D, Lee HR, Zhao W, Liu N, et al. Hierarchical nanostructured conducting polymer hydrogel with high electrochemical activity. Proc Natl Acad Sci 2012;109:9287–92. doi:10.1073/pnas.1202636109.
[81] MacDiarmid AG, Min Y, Wiesinger JM, Oh EJ, Scherr EM, Epstein AJ. Towards optimization of electrical and mechanical properties of polyaniline: Is crosslinking between chains the key? Synth Met 1993;55:753–60. doi:10.1016/0379-6779(93)90147-O.
[82] Wang Y, Shi Y, Pan L, Ding Y, Zhao Y, Li Y, et al. Dopant-Enabled Supramolecular Approach for Controlled Synthesis of Nanostructured Conductive Polymer Hydrogels. Nano Lett 2015;15:7736–41. doi:10.1021/acs.nanolett.5b03891.
[83] Xu Y, Sheng K, Li C, Shi G. Self-assembled graphene hydrogel via a one-step hydrothermal process. ACS Nano 2010;4:4324–30. doi:10.1021/nn101187z.
[84] Li J, Liu C, Liu Y. Au/graphene hydrogel: synthesis, characterization and its use for catalytic reduction of 4-nitrophenol. J Mater Chem 2012;22:8426.

doi:10.1039/c2jm16386a.
[85] Cong HP, Ren XC, Wang P, Yu SH. Macroscopic multifunctional graphene-based hydrogels and aerogels by a metal ion induced self-assembly process. ACS Nano 2012;6:2693–703. doi:10.1021/nn300082k.
[86] Rahaman M, Aldalbahi A, Govindasami P, Khanam N, Bhandari S, Feng P, et al. A New Insight in Determining the Percolation Threshold of Electrical Conductivity for Extrinsically Conducting Polymer Composites through Different Sigmoidal Models. Polymers (Basel) 2017;9:527. doi:10.3390/polym9100527.
[87] Sandler JKW, Kirk JE, Kinloch IA, Shaffer MSP, Windle AH. Ultra-low electrical percolation threshold in carbon-nanotube-epoxy composites. Polymer (Guildf) 2003;44:5893–9. doi:10.1016/S0032-3861(03)00539-1.
[88] Hunt AG. Percolation Theory. Percolation Theory Flow Porous Media 2005;674:1–31. doi:10.1007/978-3-662-02403-4_5.
[89] Last BJ, Thouless DJ. Percolation theory and electrical conductivity. Phys Rev Lett 1971;27:1719–21. doi:10.1103/PhysRevLett.27.1719.
[90] Wang W, Zhang X, Teng A, Liu A. Mechanical reinforcement of gelatin hydrogel with nanofiber cellulose as a function of percolation concentration. Int J Biol Macromol 2017;103:226–33. doi:10.1016/j.ijbiomac.2017.05.027.
[91] Wiegand N, Mäder E. Multifunctional Interphases: Percolation Behavior, Interphase Modification, and Electro-Mechanical Response of Carbon Nanotubes in Glass Fiber Polypropylene Composites. Adv Eng Mater 2016;18:376–84. doi:10.1002/adem.201500447.
[92] Grunlan JC, Mehrabi AR, Bannon M V., Bahr JL. Water-based single-walled-nanotube-filled polymer composite with an exceptionally low percolation threshold. Adv Mater 2004;16:150–3. doi:10.1002/adma.200305409.
[93] Feng Y, Ning N, Zhao Q, Liu J, Zhang L, Tian M, et al. Role of block copolymer morphology on particle percolation of polymer nanocomposites. Soft Matter 2014;00:1–9. doi:10.1039/c4sm01119h.
[94] Katunin A. Analysis of critical percolation clusters of mixtures of conducting and dielectric polymers. J Appl Math Comput Mech 2016;15:59–69. doi:10.17512/jamcm.2016.1.06.
[95] Chodak I, Krupa I. "Percolation effect" and mechanical behavior of carbon black filled polyethylene. J Mater Sci Lett 1999;18:1457–9. doi:10.1023/A:1006665527806.
[96] Adewunmi AA, Ismail S, Sultan AS. Carbon Nanotubes (CNTs) Nanocomposite Hydrogels Developed for Various Applications: A Critical Review. J Inorg Organomet Polym Mater 2016;26:717–37. doi:10.1007/s10904-016-0379-6.
[97] Meschi Amoli B, Hu A, Zhou NY, Zhao B. Recent progresses on hybrid micro–nano filler systems for electrically conductive adhesives (ECAs) applications. J Mater Sci Mater Electron 2015;26:4730–45. doi:10.1007/s10854-015-3016-1.
[98] Aktaş DK, Evingür GA, Pekcan Ö. Critical Exponents of Gelation and Conductivity in Polyacrylamide Gels Doped by Multiwalled Carbon Nanotubes. Compos Interfaces 2010;17:301–18. doi:10.1163/092764410X495243.
[99] Chen Q, Gong S, Moll J, Zhao D, Kumar SK, Colby RH. Mechanical reinforcement of polymer nanocomposites from percolation of a nanoparticle network. ACS Macro Lett 2015;4:398–402. doi:10.1021/acsmacrolett.5b00002.
[100] Liu Y, He X, Hanlon D, Harvey A, Khan U, Li Y, et al. Electrical, Mechanical, and

Capacity Percolation Leads to High-Performance MoS2/Nanotube Composite Lithium Ion Battery Electrodes. ACS Nano 2016;10:5980–90. doi:10.1021/acsnano.6b01505.
[101] Hall PJ, Mirzaeian M, Fletcher SI, Sillars FB, Rennie AJR, Shitta-Bey GO, et al. Energy storage in electrochemical capacitors: designing functional materials to improve performance. Energy Environ Sci 2010;3:1238. doi:10.1039/c0ee00004c.
[102] Conway BE. Transition from "Supercapacitor" to "Battery" Behavior in Electrochemical Energy Storage. J Electrochem Soc 1991;138:1539. doi:10.1149/1.2085829.
[103] Liu Q, Nayfeh O, Nayfeh MH, Yau ST. Flexible supercapacitor sheets based on hybrid nanocomposite materials. Nano Energy 2013;2:133–7. doi:10.1016/j.nanoen.2012.08.007.
[104] Yang Z, Deng J, Chen X, Ren J, Peng H. A Highly Stretchable, Fiber-Shaped Supercapacitor. Angew Chemie Int Ed 2013;52:13453–7. doi:10.1002/anie.201307619.
[105] Yu C, Masarapu C, Rong J, Wei BQM, Jiang H. Stretchable supercapacitors based on buckled single-walled carbon nanotube macrofilms. Adv Mater 2009;21:4793–7. doi:10.1002/adma.200901775.
[106] Ghosh D, Das CK. Hydrothermal growth of hierarchical Ni3S2and Co3S4on a reduced graphene oxide hydrogel@Ni foam: A high-energy-density aqueous asymmetric supercapacitor. ACS Appl Mater Interfaces 2015;7:1122–31. doi:10.1021/am506738y.
[107] Hu L, Pasta M, La Mantia F, Cui L, Jeong S, Deshazer HD, et al. Stretchable, porous, and conductive energy textiles. Nano Lett 2010;10:708–14. doi:10.1021/nl903949m.
[108] Zeng S, Chen H, Cai F, Kang Y, Chen M, Li Q. Electrochemical fabrication of carbon nanotube/polyaniline hydrogel film for all-solid-state flexible supercapacitor with high areal capacitance. J Mater Chem A 2015;3:23864–70. doi:10.1039/C5TA05937B.
[109] Li W, Lu H, Zhang N, Ma M. Enhancing the properties of conductive polymer hydrogels by freeze-thaw cycles for high-performance flexible supercapacitors. ACS Appl Mater Interfaces 2017;9:20142–9. doi:10.1021/acsami.7b05963.
[110] Wang K, Zhang X, Li C, Sun X, Meng Q, Ma Y, et al. Chemically Crosslinked Hydrogel Film Leads to Integrated Flexible Supercapacitors with Superior Performance. Adv Mater 2015;27:7451–7. doi:10.1002/adma.201503543.
[111] Zhang L, Shi G. Preparation of Highly Conductive Graphene Hydrogels for Fabricating Supercapacitors with High Rate Capability. J Phys Chem C 2011;115:17206–12. doi:10.1021/jp204036a.
[112] Wu Y, Liu S, Zhao K, Yuan H, Lv K, Ye G. Facile Synthesis of 3D Graphene Hydrogel/Carbon Nanofibers Composites for Supercapacitor Electrode. ECS Solid State Lett 2015;4:M23–5. doi:10.1149/2.0031512ssl.
[113] Xu Y, Lin Z, Huang X, Wang Y, Huang Y, Duan X. Functionalized graphene hydrogel-based high-performance supercapacitors. Adv Mater 2013;25:5779–84. doi:10.1002/adma.201301928.
[114] Xu Y, Lin Z, Huang X, Liu Y, Huang Y, Duan X. Flexible Solid-State Supercapacitors Based on Three-Dimensional Graphene Hydrogel Films. ACS Nano 2013;7:4042–9. doi:10.1021/nn4000836.
[115] Chen P, Yang JJ, Li SS, Wang Z, Xiao TY, Qian YH, et al. Hydrothermal synthesis of macroscopic nitrogen-doped graphene hydrogels for ultrafast supercapacitor. Nano Energy 2013;2:249–56. doi:10.1016/j.nanoen.2012.09.003.
[116] Wang Y, Yang X, Pandolfo AG, Ding J, Li D. High-Rate and High-Volumetric Capacitance of Compact Graphene-Polyaniline Hydrogel Electrodes. Adv Energy Mater 2016;6:1600185. doi:10.1002/aenm.201600185.

[117] Mao L, Guan C, Huang X, Ke Q, Zhang Y, Wang J. 3D Graphene-Nickel Hydroxide Hydrogel Electrode for High-Performance Supercapacitor. Electrochim Acta 2016;196:653–60. doi:10.1016/j.electacta.2016.02.084.
[118] Yang Y, Liang Y, Zhang Y, Zhang Z, Li Z, Hu Z. Three-dimensional graphene hydrogel supported ultrafine RuO 2 nanoparticles for supercapacitor electrodes. New J Chem 2015;39:4035–40. doi:10.1039/C5NJ00062A.
[119] Zhang H, Xie A, Wang C, Wang H, Shen Y, Tian X. Bifunctional reduced graphene oxide/V2O5 composite hydrogel: Fabrication, high performance as electromagnetic wave absorbent and supercapacitor. ChemPhysChem 2014;15:366–73. doi:10.1002/cphc.201300822.
[120] Pattananuwat P, Aht-ong D. Controllable morphology of polypyrrole wrapped graphene hydrogel framework composites via cyclic voltammetry with aiding of poly (sodium 4-styrene sulfonate) for the flexible supercapacitor electrode. Electrochim Acta 2017;224:149–60. doi:10.1016/j.electacta.2016.12.036.
[121] Zhang N, Fu C, Liu D, Li Y, Zhou H, Kuang Y. Three-Dimensional Pompon-like MnO 2 /Graphene Hydrogel Composite for Supercapacitor. Electrochim Acta 2016;210:804–11. doi:10.1016/j.electacta.2016.06.004.
[122] Pattananuwat P, Aht-Ong D. One-step method to fabricate the highly porous layer of poly (pyrrole/ (3, 4-ethylenedioxythiophene)/) wrapped graphene hydrogel composite electrode for the flexibile supercapacitor. Mater Lett 2016;184:60–4. doi:10.1016/j.matlet.2016.08.031.
[123] Xiang X, Zhang W, Yang Z, Zhang Y, Zhang H, Zhang H, et al. Smart and flexible supercapacitor based on a porous carbon nanotube film and polyaniline hydrogel. RSC Adv 2016;6:24946–51. doi:10.1039/C6RA00705H.
[124] Ghosh S, Inganäs O. Conducting Polymer Hydrogels as 3D Electrodes: Applications for Supercapacitors. Adv Mater 1999;11:1214–8. doi:0935-9648/99/1410-1214.
[125] Li W, Gao F, Wang X, Zhang N, Ma M. Strong and Robust Polyaniline-Based Supramolecular Hydrogels for Flexible Supercapacitors. Angew Chemie Int Ed 2016;55:9196–201. doi:10.1002/anie.201603417.
[126] Huang Y, Li H, Wang Z, Zhu M, Pei Z, Xue Q, et al. Nanostructured Polypyrrole as a flexible electrode material of supercapacitor. Nano Energy 2016;22:422–38. doi:10.1016/j.nanoen.2016.02.047.
[127] Stephan AM. Review on gel polymer electrolytes for lithium batteries. Eur Polym J 2006;42:21–42. doi:10.1016/j.eurpolymj.2005.09.017.
[128] Xu K. Nonaqueous liquid electrolytes for lithium-based rechargeable batteries. Chem Rev 2004;104:4303–417. doi:10.1021/cr030203g.
[129] Long JW, Dunn B, Rolison DR, White HS. Three-dimensional battery architectures. Chem Rev 2004;104:4463–92. doi:10.1021/cr020740l.
[130] Palacín MR. Recent advances in rechargeable battery materials: a chemist's perspective. Chem Soc Rev 2009;38:2565. doi:10.1039/b820555h.
[131] Novák P, Müller K, Santhanam KS V., Haas O. Electrochemically Active Polymers for Rechargeable Batteries. Chem Rev 1997;97:207–82. doi:10.1021/cr941181o.
[132] Cheng F, Liang J, Tao Z, Chen J. Functional materials for rechargeable batteries. Adv Mater 2011;23:1695–715. doi:10.1002/adma.201003587.
[133] Winter M, Besenhard JO, Spahr ME, Novák P. Insertion Electrode Materials for Rechargeable Lithium Batteries. Adv Mater 1998;10:725–63. doi:10.1002/(SICI)1521-

4095(199807)10:10<725::AID-ADMA725>3.0.CO;2-Z.
[134] Kiani MA, Mousavi MF, Rahmanifar MS. Synthesis of nano- and micro-particles of LiMn2O4: Electrochemical investigation and assessment as a cathode in li battery. Int J Electrochem Sci 2011;6:2581–95. doi:10.1039/c1ee01598b.
[135] Goodenough JB, Kim Y. Challenges for rechargeable Li batteries. Chem Mater 2010;22:587–603. doi:10.1021/cm901452z.
[136] Zhou G, Li F, Cheng H-M. Progress in flexible lithium batteries and future prospects. Energy Environ Sci 2014;7:1307–38. doi:10.1039/C3EE43182G.
[137] Cheng J, Gu G, Ni W, Guan Q, Li Y, Wang B. Graphene oxide hydrogel as a restricted-area nanoreactor for synthesis of 3D graphene-supported ultrafine TiO 2 nanorod nanocomposites for high-rate lithium-ion battery anodes. Nanotechnology 2017;28:305401. doi:10.1088/1361-6528/aa77c6.
[138] Nishide H, Oyaizu K. MATERIALS SCIENCE: Toward Flexible Batteries. Science (80-) 2008;319:737–8. doi:10.1126/science.1151831.
[139] Wu H, Yu G, Pan L, Liu N, McDowell MT, Bao Z, et al. Stable Li-ion battery anodes by in-situ polymerization of conducting hydrogel to conformally coat silicon nanoparticles. Nat Commun 2013;4:1943–6. doi:10.1038/ncomms2941.
[140] Liu B, Soares P, Checkles C, Zhao Y, Yu G. Three-dimensional hierarchical ternary nanostructures for high-performance Li-ion battery anodes. Nano Lett 2013;13:3414–9. doi:10.1021/nl401880v.
[141] Zhang M, Wang Y, Jia M. Three-Dimensional Reduced Graphene Oxides Hydrogel Anchored with Ultrafine CoO Nanoparticles as Anode for Lithium Ion Batteries. Electrochim Acta 2014;129:425–32. doi:10.1016/j.electacta.2014.02.097.
[142] Liu J, Zhang Q, Wu Z-Y, Wu J-H, Li J-T, Huang L, et al. A high-performance alginate hydrogel binder for the Si/C anode of a Li-ion battery. Chem Commun 2014;50:6386. doi:10.1039/c4cc00081a.
[143] Chen Z, To JWF, Wang C, Lu Z, Liu N, Chortos A, et al. A three-dimensionally interconnected carbon nanotube-conducting polymer hydrogel network for high-performance flexible battery electrodes. Adv Energy Mater 2014;4:1–10. doi:10.1002/aenm.201400207.
[144] Zhou T, Gao X, Dong B, Sun N, Zheng L. Poly(ionic liquid) hydrogels exhibiting superior mechanical and electrochemical properties as flexible electrolytes. J Mater Chem A 2016;4:1112–8. doi:10.1039/C5TA08166A.
[145] Lyu F, Yu S, Li M, Wang Z, Nan B, Wu S, et al. Supramolecular hydrogel directed self-assembly of C- and N-doped hollow CuO as high-performance anode materials for Li-ion batteries. Chem Commun 2017;53:2138–41. doi:10.1039/C6CC09702B.

Figure Captions

Figure 1. Electrically conductive hydrogels are an emerging class of hydrogels combining a hydrophilic matrix with conductive fillers, and they have exceptional promises in a wide range of applications.

Figure 2. Four main approaches used to obtain ECAs: (1) Hydrogel formation from a conductive filler suspension; (2) Polymerization within a preformed hydrogel matrix; (3) Crosslinking conductive polymers by dopant molecules; (4) Self-assembly of Graphene Hydrogel via Supramolecular Interactions.

Figure 3. Schematic of mussel-inspired PDA-rGO/PAM hydrogel. Step 1: dopamine pre-polymerization; Step 2: GO was partially reduced to form rGO; Step 3: polymerization of acrylamide monomers. Adapted with permission from Ref. 73. Copyright © 2017 Wiley-VCH Verlag GmbH & Co. KGaA, Weinheim.

Figure 4. Synthetic approach of heparin-methacrylate/PANI hydrogel. Adapted with permission from Ref. 28. Copyright © 2014 American Chemical Society.

Figure 5. (a) Schematic illustrations of the 3D hierarchical microstructure of the PANI hydrogel; Adapted with permission from Ref. 80. Copyright © 2012 National Academy of Sciences. (b) Controlled synthesis of the CuPcTs doped PPy hydrogel. Adapted with permission from Ref. 82. Copyright © 2015 American Chemical Society.

Figure 6. (a) Photograph of GO dispersion before (left) and after hydrothermal reduction (right). (b) The hydrothermal formation mechanism for the graphene hydrogel. (c) Optical images of the graphene hydrogels prepared by hydrothermal reduction at different GO concentration. (d) Optical images of three graphene hydrogel columns holding 100 g weight. Adapted with permission from Ref. 83. Copyright © 2010 American Chemical Society.

Figure 7. (a) Distance distribution of the conductive fillers in an insulting matrix; Adapted with permission from Ref. 90. (Open Access Journal). (b) Conceptual graph showing the change in conductance as a function of the concentration of conductive fillers.

Figure 8. (a) CV curves of the PANI hydrogel electrode at different scan rates. Adapted with permission from Ref. 80. Copyright © 2012 National Academy of Sciences. (b) Specific capacitance of PPy electrodes with different material loadings at different current densities. (c) Cycling performance of PPy electrodes over 3000 charge-discharge cycles. Adapted with permission from Ref. 50. Copyright © 2014 The Royal Society of Chemistry.

Figure 9. (a) The tensile stress-strain curve of PANI hydrogel; (b) The compression stress-stain curve of PANI hydrogel; (c) Schematic structure of a flexible solid-state supercapacitor made by PANI hydrogel electrode; (d) CV tests at scan rates of 10-100 m/V. (e) Specific capacitance of the PANI supercapacitor at varied GCD current densities; (f) Capacitance retention of the supercapacitor after 1000 mechanical folding cycles with 180 bending. Adapted with permission from Ref. 125. Copyright © 2016 WILEY-VCH Verlag GmbH & Co. KGaA, Weinheim.

Figure 10. (a) Schematic of graphene hydrogel-based supercapacitor device; (b) CV curves of the supercapacitor at different scan rates; Adapted with permission from Ref. 83. Copyright © 2010 American Chemical Society. (c) Plot of specific capacitance versus discharging current density for hydrazine reduced graphene hydrogel electrode; (d) Cycling stability of the electrode upon charging/discharging at a current density of 4 A/g. Adapted with permission from Ref. 110. Copyright © 2011 American Chemical Society.

Figure 11. (a) Digital photograph of a standing graphene hydrogel electrode; (b) Schematic diagram of the solid-state flexible supercapacitor with graphene hydrogels as the electrode and H2SO4-PVA polymer gel as the electrolyte; (c) CV curves at 10 mV/s and (d) specific capacitances of the graphene hydrogel electrodes in H2SO4-PVA gel electrolyte and in 1M H2SO4 aqueous electrolyte; (e) CV curves of the supercapacitor at 10 mV/s with different bending angles; (d) Cycling stability of the solid-state supercapacitor under 1000 bending cycles. Adapted with permission from Ref. 113. Copyright © 2013 WILEY-VCH Verlag GmbH & Co. KGaA, Weinheim.

Figure 12. (a) TEM image of TiO2 nanosphere decorated graphene hydrogel; (b) CV curves for the TiO2 nanosphere decorated graphene hydrogel electrode and the graphene hydrogel electrode at the same scan rate of 5 mV/s; (c) Charge/discharge cycling test of the TiO2 nanosphere decorated graphene hydrogel electrode. Adapted with permission from Ref. 79. Copyright © 2013 American Chemical Society. (d) TEM image of the rGO/V2O5 composite hydrogel; (e)GCD curves of the rGO/V2O5 hydrogel electrode measured at different current densities; (f) Cycling stability of the rGO/V2O5 composite hydrogel electrode at a current density of 1.0 A/g over 1000 cycles. Adapted with permission from Ref. 119. Copyright © 2014 Wiley-VCH Verlag GmbH & Co. KGaA, Weinheim.

Figure 13. (a) Schematic illustration of 3D porous Si-PANI hydrogel composite; (b) CV curves of both PANI hydrogel and Si-PANI hydrogel electrodes at a scan rate of 0.1 mV/s; (c) Electrochemical cycling performance of the in-situ polymerized and simply mixed Si-PANI composite electrodes, and pure silicon electrode under charge/discharge cycles; (d) Lithiation/delithiation capacity and coulombic efficiency of Si-PANI electrode cycled at current density of 6.0 A/g for 5,000 cycles; (e) Galvanostatic charge/discharge profiles plotted for the 1st, 1000th, 2000th, 3000th and 4000th cycles. Adapted with permission from Ref. 139. Copyright © 2013 Macmillan Publishers Limited.

Figure 14. (a) Ternary electrode structure: Si/PPy/CNT; (b) SEM image of Si/PPy/CNT hierarchical hydrogel; (c) Nyquist plots of the hybrid electrode in the frequency range between 0.1 Hz and 1 MHz; (d) CV curve of the Si/PPy/CNT electrode at a scanning rate of 0.1 mV/s; (e) Voltage profiles of Si/PPy/CNT electrode; (f) Discharge capacity and Coulombic efficiency of the Si/PPy/CNT electrode. Adapted with permission from Ref. 140. Copyright © 2013 American Chemical Society.

Figure 15. (a) Schematic illustration of the aqueous solution process to fabricate PEDOT:PSS/CNT flexible electrodes; (b) SEM image of the TiO2-PEDOT:PSS-CNT film electrode; (c) Resistance of the TiO2-PEDOT:PSS-CNT electrode over 500 bending cycles with

a bending radius of 3.5 mm; (d) Capacity dependence of each electrode versus charging time. Adapted with permission from Ref. 143. Copyright © 2014 WILEY-VCH Verlag GmbH & Co. KGaA, Weinheim.